

Response to Reviewers

We thank the reviewers for their detailed comments and helpful suggestions. We have addressed each comment below, with the Referee comment in **bold italicized text**, our response in plain text, and any manuscript changes noted in **blue text**. In addition, the revised manuscript with changes marked up has been attached to the end of our response to reviewers.

Reviewer # 1

Comments:

Zhang et al. present a new experimental setup measuring glass transition temperature (T_g) using dielectric spectroscopy of thin films. Aerosol particles are deposited on an interdigitated electrode device using an electrostatic precipitator, eventually forming a thin film. The authors propose a new data analysis approach using the broadband dielectric spectroscopy data to determine T_g . The advantage of the technique compared to more traditional calorimetric techniques is that it needs considerably less material, hence it may open the possibility to measure ambient aerosol. Clearly, that makes the paper important and well suited to be published in AMT. The authors use two surrogates for secondary organic aerosol (SOA) to demonstrate that their technique yields glass transition temperatures comparable to reference methods. Both are pure compounds (glycerol and citric acid), no simple mixture nor an aqueous solution was investigated.

However, as one of the two tests (citric acid) show quite substantial deviation in measured T_g (307 K) compared to what is measured with calorimetric techniques (281- 285 K) -when the data are analyzed using the new technique - there is little evidence (namely, only the glycerol data) that the technique will actually work for ambient or laboratory SOA particles. As there are ample data available for pure compound SOA surrogates, aqueous SOA surrogates, as well as for simple mixtures [e.g. Lienhard et al., 2012; Dette et al., 2015; Dette and Koop, 2015], I think it is essential to perform measurements on more pure component surrogates, at least one mixture and – if possible – also an aqueous surrogate to characterize the experimental setup. As it is now, the paper does not allow the reader to judge whether the technique is actually feasible or needs further improvements before being applied to samples of unknown T_g .

We thank the reviewer for reading and reviewing our manuscript, as well as his/her feedback. The reviewer brings up an excellent point of why we chose to use glycerol in this study. Glycerol is commonly used as a compound for characterizing and calibrating the performance of the dielectric spectroscopy. If the dielectric results of glycerol at all temperatures and all frequencies match the previous literature, then the dielectric spectrometer is considered calibrated and all other compounds that have dielectric spectra should show similar results. As shown in Figure 3, the dielectric measurements of glycerol in our studies match the previous studies very well, showing that the dielectric spectrometer in our study is accurate and is able to give accurate results. We also added a new plot comparing the data from the literature with this work at several different temperatures, as shown in Figure S1. The results match very well. We added the following text to further validate this method.

“The comparison of the dielectric relaxation timescale of glycerol measured from this study with literature values is shown in Figure S1, for several different temperatures. The results show that our measurements match the previously published results in the super-Arrhenius region when the compound is in equilibrium at a given temperature, with almost identical values. As the temperature continues to drop, glycerol and other compounds we tested fall out of equilibrium and become glass, which exhibits Arrhenius behavior. The transition from super-Arrhenius to Arrhenius behavior in this study provides the kinetically controlled glass transition as the compounds change from liquid to glassy state.”

We understand the reviewer’s interests to see more results to further validate this method. We acknowledged the work by previous publications (Dette et al., 2014; Lienhard et al., 2014; Dette and Koop, 2015) in the manuscript and examined three additional organic aerosols that have known glass transition temperatures, and the results from this study agree with literature values. We added text and plots in the main manuscript to include the above results.

“Glycerol, 1,2,6-hexanetriol, di-n-butyl phthalate, dioctyl phthalate, and citric acid particles were generated through the homogeneous nucleation method and atomizer method, respectively. The measured dielectric spectra of each compound show distinct relationships of their dielectric relaxation timescales with a 5 K/min cooling rate, as shown in Figure 5.

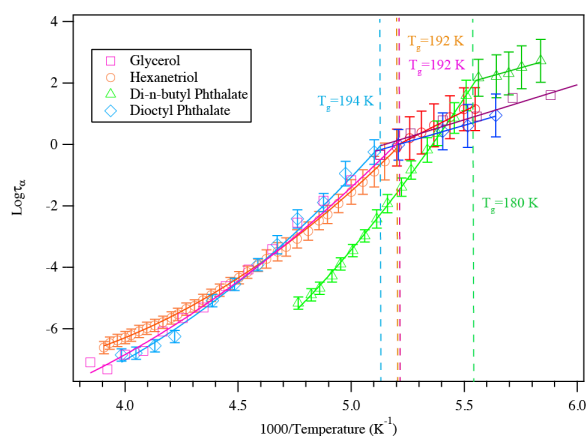


Figure 5. A plot of superimposed data points and curves constructed for glycerol, 1,2,6-hexanetriol, di-n-butyl phthalate, and dioctyl phthalate cooled at 5K/min. The solid color lines represent the fitted curves for the super-Arrhenius and Arrhenius region. The intersection between the two lines indicates the kinetically controlled glass transition region for each compound. The glass transition at a 5K/min cooling rate for each compound is shown in the plot.”

The focus of this manuscript is to show that the thin film technique coupled with the dielectric spectroscopy is able to provide kinetically controlled glass transition results for submicron organic aerosol particles, and that cooling rates can affect the glass transition. However, whether this technique is fully applicable to all types of mixtures, aqueous aerosol systems, and even ambient aerosols, is currently being investigated by our team and is not within the scope of this manuscript. We added the following text to illustrate the future directions for this study. “Future

research needs to be performed to examine organic mixtures and even secondary organic aerosols (SOA) using this method.”

Detailed comments:

1 Introduction:

I suggest add a paragraph explaining that one important property needed to understand kinetic limitations in gaseous uptake or loss of compounds in atmospheric aerosol particles is the diffusivity of this compound in the condensed phase. Measuring T_g of ambient SOA will indicate that below/at this temperature kinetic limitations will occur, but it does not give immediate quantitative insight.

We thank the reviewer for this comment. The reason why we did not add this part earlier, just as the reviewer pointed out, was due to the fact that the glassy state is not a good guideline for kinetic limitations, as particles in certain semi-solid states can also impose kinetic limitations on the uptake and multiphase reaction of gas phase species. But it is an important motivation for studying phase states, and therefore we added new text to explain the effect of the glassy phase state on kinetic limitations.

“The phase state of aerosol particles also influences the diffusion of the gas phase species into the atmosphere, affecting the oxidation extent and multiphase reactions of the particles. For example, Shiraiwa and Seinfeld (2012) used models to predict that when aerosol particles are in certain semi-solid and glassy phase states, the reactive uptake of gas phase species will be kinetically limited. Kuwata and Martin (2012) showed that the phase state of secondary organic aerosols (SOA) affects the uptake of ammonia into the particles. Zhang et al. (2018) provided experimental and modeling evidence that the reactive uptake of isoprene-derived epoxydiols (IEPOX) into acidic sulfate particles is influenced by the phase state, which can contribute to at least a 30% reduction of isoprene-derived SOA in the Southeast U.S.”

Technical comment: Page 3, line 60: “nucleate” seems not the right wording here, better use “become activated” or similar.

We thank the reviewer for this comment. “Nucleate” has been changed to “have liquid water condense on them”

2 Experimental Setup:

One information missing is how much aerosol mass is needed for producing the film on the device. At least the area of the device and the approximate film thickness should be given. Even better, if the authors can provide the mass concentration in the aerosol flow prior to the precipitator and the time needed to accumulate for forming the film on the device.

We added the following text in the manuscript to address the reviewer’s comment. “The volume concentration of the aerosol particles at the inlet of the precipitator was $4.5 \times 10^{11} \text{ nm}^3 \text{ cm}^{-3}$. After collecting for 5 hours, the film thickness is estimated to be 1-2 μm on 1 mm \times 8 mm substrate

based on the difference of volume concentration between the inlet and the outlets of the precipitator, the flow rate, the collection time, and assuming 50% collection efficiency.

3 Data analysis:

I do not see the advantage of not adding the information of the SI into the main text. Please. Incorporate it including the raw data of Fig. S1 into section 3.1.

We moved the Figure S1 to section 3.1 and named it Figure 6. We also added the following text in the main text to call out Figure 6.

“The kinetically controlled dielectric spectra fitted using Eq. (S2) are shown in Figure 6. From the fitting results in Figure 6, the dielectric relaxation timescales τ are derived as a function of temperature, as shown in Figure 7.

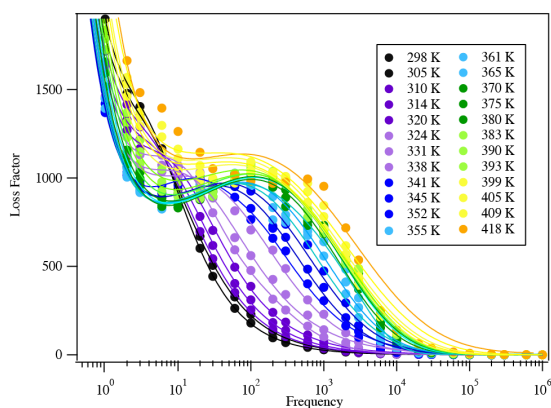


Figure 6. The dielectric relaxation spectrum of citric acid at different temperatures. The solid circles are measured experimental data and the solid lines are fitting curves parameterized from Eq. (S2) and Adrjanowicz et al. (2009).”

I also find section 3.2 difficult to read as a non-expert. How does the discussion here connect to the issues of determining “fragility” [e.g. Angell, 2002]? I am not convinced that the glass community agrees that the intercept shown in Fig. 4 is the “true” glass transition.

We thank the reviewer for the comment. Fragility, as described in Angell et al. (2002), is a parameter used to characterize the steepness of the slow down of the dynamics of glass-forming liquids as temperature is decreased. In this paper, we use dynamical facilitation theory as the scientific basis of the study, which is known to capture the behavior of various liquids over a large range of fragilities. According to this theory, the analog of the steepness, i.e., the curvature of the log relaxation time versus inverse temperature curve, is a parameter J , which is described in section 3.2 of the main text. J is unique to each material and can be related to the rate of motion of individual molecules (Keys et al., 2013). We added the following text to explain the theory in detail.

“The method used in our studies is based on dynamical facilitation theory (Elmatad et al., 2009; Chandler and Garrahan, 2010; Keys et al., 2011; Keys et al., 2013; Hudson, 2015, Hudson and Mandadapu, 2018), which also takes into account the effect of cooling rate on the glass transition. According to this theory, as a compound is cooled and transitions from a liquid to a supercooled liquid it exhibits super-Arrhenius behavior given by the following equation:

$$\log \tau/\tau_0 = J^2(1/T - 1/T_0)^2 \quad (3)$$

where J is an energy scale intrinsic to each material related to the rate of motion of individual molecules, T_0 is termed the “onset temperature” and refers to the temperature at which a liquid showing Arrhenius relaxation becomes a supercooled liquid showing super-Arrhenius relaxation, and τ_0 is a temperature-independent reference time scale of the order of the time taken for molecules to locally rearrange (Keys et al., 2011)”

Further, the idea of using the intersection between the super-Arrhenius and Arrhenius regions to determine glass transition temperature as a compound is cooled or warmed has been discussed and supported by publications from various research groups (Saiter et al., 2007; Shinyashiki et al., 2008). The predictions of the physical chemistry theory behind this idea, i.e., dynamical facilitation theory, agrees well with laboratory experiments (Keys et al., 2013).

The traditional method used $\tau=100$ s as the glass transition temperature, because the experiments were performed at equilibrium, i.e., the temperature of the chamber is set to one value, and then changed to the next one. Because those compounds are always measured at equilibrium, it is difficult to observe the transition from super-Arrhenius to Arrhenius regimes. Recently studies have shown that τ need not always be 100 s for all liquids (Saiter et al., 2007; Bahous et al., 2014) and the dielectric spectroscopy community does mostly agree that intersection between the two regimes reflects the kinetically controlled T_g more accurately (Saiter et al., 2007; Shinyashiki et al., 2008). Therefore we respectfully disagree with the reviewer: the intersection between the two regimes as an indication of the “true” glass transition is one of the methods used in the literature to determine the value of the glass transition. We use this technique to determine the glass transition temperature because it has a theoretical basis in dynamical facilitation theory, and does not involve an empirical or arbitrary reference point such as $\tau=100$ s for the determination of the glass transition.

Fig. 4: The caption needs to say which material is shown. Or, is this just a sketch to show the idea? Instead of “given cooling rate” in the legend, the actual cooling rate should be provided. They are no error bars shown for the data points: Are these actually the measurements, or some points arbitrarily taken from the fits? You need to provide more detail here.

Figure 4 is an arbitrary plot for illustration purposes, not real measurement. To clarify, we have added the following text:

“Figure 4 shows a typical relationship between the dielectric relaxation timescale and the temperature, as a compound is cooled down or warmed up between the liquid state and glassy state.”

We also changed the caption for Figure 4:

“Figure 4. An illustrated plot of the relationship between dielectric relaxation time scale and temperature. The logarithm of the relaxation is plotted against inverse T, i.e., $\log \tau$ vs $1000/T$. By linking the data points together, one can plot the super-Arrhenius curve (red) and the Arrhenius line (green). Using a consistent cooling rate, the intersection of the two regions identifies the compound’s glass transition temperature, as indicated by the shaded blue region. The intersection of the two black lines represents the glass transition point. The intersection of the two black dashed lines shows the glass transition temperature determined using traditional method when $\tau=100$ s.”

4 Results and discussion:

First, there is more data available in the literature to compare your data with: for glycerol see for example Lienhard et al. (2012). Citric acid has been measured by Lienhard et al. [2012] as well and by Dette et al. [2014].

We thank the reviewer for the comment. We have included the references that the reviewer provided. However, we would like to point out that these studies use calorimetry for their measurements in contrast with our dielectric relaxation spectroscopy measurements. Studies have shown that the glass transition temperature can change significantly between these techniques, by 5-10 K or sometimes even up to 50 K (Angell, 2002; Shinyashiki et al., 2008), making comparison difficult.

Second, in Fig. 5 you determined Tg of citric acid as 305-315 K, whereas in Table 1 you write 307+/-5 K. Please check.

We thank the reviewer for the comment. We have examined the data and updated it to be 302-312K, as shown below:

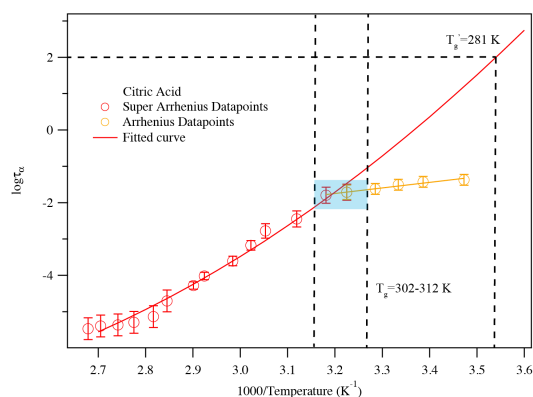


Figure 7. A plot of superimposed data-points and curves constructed for citric acid warmed at 5K/min. The solid color lines represent the fitted curves for the super-Arrhenius and Arrhenius region. The blue shaded area shows the glass transition region. The two vertical black lines associated with the blue shaded area indicate the corresponding temperature range where the super Arrhenius curve intersects with the Arrhenius line. The traditional glass transition temperature, i.e., the temperature when $\tau=100$ s, is also marked.

Obviously, Fig. 5 shows a very significant difference when comparing the “classical” determination ($\tau = 100\text{s}$) for T_g (281 K) and your new method (305-315 K). As the former agrees with the calorimetric measurements of numerous experiments in the literature, whereas the latter show significant deviation, you definitely need more evidence than provided to support the new method. At present, the reader will conclude that the new method is not reliable.

We thank the reviewer for the comment. We understand the reviewer’s concern. We would like to respectfully point out that using the intercept to determine the glass transition is not a “new” method. The theory and related discussions of its advantages have been published previously by multiple research groups (Keys et al., 2013; Bahous et al., 2014; Limmer and Chandler, 2014; Hudson, 2015). Within the dielectric relaxation method, the difference between using $\tau=100$ s and the intercept method is that one measures the equilibrium state between the compound and the temperature, while the latter measures the dynamic process with various cooling or heating rates (Saiter et al., 2007; Bahous et al., 2014).

We would also like to point out the DSC method and the dielectric method do not have to be in exact agreement. Due to the differences in measurement parameters and definitions of the glass transition, different measurements can give different T_g values (Shinyashiki et al., 2008). DSC uses heat capacity to measure the glass transition while dielectric relaxation uses molecular variations to define the glass transition. Angell (2012) also pointed out in his paper that there are at least three different definitions of the glass transition and the T_g determined by each can be 50 K different from each other.

To include more evidence, we now show data for three other compounds besides glycerol and citric acid, and the results show very good agreement with the previous studies, not just for T_g measurement (as shown in Table 1, which could depend on the definition used), but also for the dielectric spectra at each temperature (Figure S1 in the SI and Figure 5 in the main text). The additional results further validate the results from our method. Please see the revised text, table, and figure below with additional data.

“As is shown in Table 1, the kinetically controlled glass transition data agree well with previously measured literature values of glycerol (Zondervan et al., 2007; Chen et al., 2012; Amann-Winkel et al., 2013), 1,2,6-hexanetriol (Nakanishi and Nozaki, 2010), di-n-butyl phthalate (Dufour et al., 1994), dioctyl phthalate (Beirnes Kimberley and Burns Charles, 2003), within 3% of the literature value. The comparison of the dielectric relaxation timescale of glycerol measured from this study with literature values is shown in Figure S1, for several different temperatures. The results show that our measurements match the previously published results in the super-Arrhenius region when the compound is in equilibrium with the temperature, with almost identical values.

Table 1. Glass transition temperatures for selected organic species at selected cooling or heating rates measured by broadband dielectric spectroscopy with a thin-film interdigitated electrode array

Compound	Chemical Formula	T _g (K)-Measured	T _g (K)-Literature
Glycerol	C ₃ H ₈ O ₃	<189 K (2 K/min)	190 K (Zondervan et al., 2007)
		192 ± 2 K (5 K/min)	191 K (Chen et al., 2012)
		194 ± 2 K (10 K/min)	196 K (Amann-Winkel et al., 2013) 191.7 ± 0.9 K (Lienhard et al., 2012)
1,2,6-hexanetriol	C ₆ H ₁₄ O ₃	192 ± 2 K (5 K/min)	196 K (Nakanishi and Nozaki, 2010)
di-n-butyl phthalate	C ₁₆ H ₂₂ O ₄	180 ± 2 K (5 K/min)	174 K (Dufour et al., 1994)
dioctyl phthalate	C ₂₄ H ₃₈ O ₄	194 ± 2 K (5 K/min)	190 K (Beirnes Kimberley and Burns Charles, 2003)
Citric Acid	C ₆ H ₈ O ₇	307 ± 5 K (5 K/min)	281 ± 5 K (Bodsworth et al., 2010)*
			285 ± 0.2 K (Lu and Zografis, 1997)
			281.9 ± 0.9 K (Lienhard et al., 2012)
			283-286 K (Dette et al., 2014)
			260 ± 10 K (Murray, 2008)**

* The data was based on modeling result. ** The data was based on fitting extrapolation result.

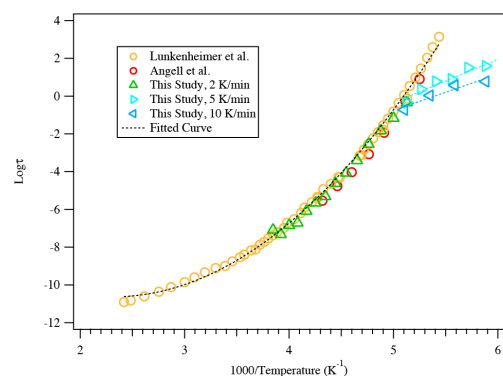


Figure S1. The logarithm of the relaxation timescale as a function of the inverse temperature derived from glycerol. The circles are from Lunkenheimer et al. (1999) and Angell (1995). The triangular points are experimental measurements from this work with different cooling rates. The dashed lines are the fitted curves for the super-Arrhenius and Arrhenius regions. The results show that the T_g values from this work match very well with previous studies.”

For citric acid, comparison of both the dielectric spectra as well as the derived T_g with literature values using the same method is difficult because there have not been any other dielectric relaxation experiments on citric acid published to our knowledge. The studies we have compared with are calorimetry measurements. It has been shown that the glass transition temperature can vary significantly depending on the experimental technique used, as well as the cooling or heating rates (Angell, 2002). Furthermore, the data shown for citric acid were obtained during a heating protocol, which can be significantly different from data obtained during a cooling

protocol due to hysteresis. Finally, it is likely that citric acid is a less fragile liquid, i.e., the glass transition temperature depends strongly on cooling or heating rates. One example of such a compound is borosilicate. Moynihan et al. (1974) show that a change of 2 K/min to 10 K/min cooling rate could change the glass transition temperature of borosilicate glass by 15 K.

Since we have found no publications presenting the dielectric spectra of citric acid, we believe that our results are worth publishing here. However, we include the following text in section 4.1 to discuss the difference in the measurements and the literature.

“(1) To date there have been no measurements of the dielectric spectra for citric acid to our knowledge. The references in Table 1 are based on DSC measurements, which may not be in exact agreement with the dielectric measurement. Angell (2012) pointed out that there are at least three different definitions of the glass transition and the T_g determined by each can be 50 K different from each other. DSC uses heat capacity change to measure the glass transition while dielectric relaxation uses molecular movements to define the glass transition. Due to the difference in measurement parameters and the definition of the glass transition, these two measurements can provide different T_g values of the same compound by up to 10 K (Shinyashiki et al., 2008). (2) This study focuses the kinetically controlled glass transition temperature at a given cooling rate, i.e., the transition of the long range intermolecular movements of the sample to determine the glass transition temperature. If the more conventional method, i.e. fitting the super-Arrhenius curve to obtain the glass transition temperature in when $\tau=100$ s, is applied to the data, as shown in Figure 7, the obtained glass transition temperature would be 281 ± 3 K, which is within 1% difference compared with the two nearest literature values. However, as previous publications have pointed out (Keys et al., 2013; Bahous et al., 2014; Limmer and Chandler, 2014; Hudson, 2018), using the transition from super-Arrhenius to Arrhenius region is likely to reflect the true glass transition when taking kinetic factors, such as cooling/heating rates, into consideration. (3) Moreover, glass transition data of citric acid are rather limited and there are differences between each study. For instance, from the literature data, the differences between three reported glass transition temperatures are up to 10%, which is the same value comparing our data to the other two nearest literature results. (4) The heating and cooling rates may also contribute to the difference of the T_g of citric acid between the literature and this study, as this study uses a lower cooling rate than the ones reported by the literature. Moynihan et al. (1974) reported that a change of 2 K/min to 10 K/min cooling rate could alter the glass transition temperature of borosilicate by 15 K. It is possible that citric acid is a less fragile liquid, similar to borosilicate, i.e., the glass transition temperature depends strongly on cooling or heating rates.”

Concerning the influence of cooling rates, I recommend to the authors to make use of the detailed study of Simatos et al. [1996], do an additional experiment using sorbitol or fructose with the setup, and compare the results with those of Simatos et al. [1996].

We thank the reviewer for pointing out the Simatos et al. paper. We have included it in our manuscript. Simatos et al. shows that T_g changes about 3-5K as the cooling rate changes from 2 K/min to 10 K/min. Unfortunately, sorbitol or fructose have relatively small dipole moments, making it very difficult to perform dielectric analysis for our current instrumental sensitivity. However, the change of 3-5 K reported in Simatos et al. agrees well with our study. Herein, we included the text to discuss this agreement reported by Simatos et al.

“This study reports an increase of 5 K or more in the glass transition of glycerol as the cooling rate changes from 2 K/min to 10 K/min. The reported increase in glass transition temperature during these cooling rates agrees with the behavior of sorbitol and fructose in another study performed by Simatos et al. (1996), which also measured the dependence of glass transition temperature on cooling rate with small organic molecules.”

Reviewer # 2

Comments:

This study developed a method to measure the kinetically-controlled glass transition temperatures using the broadband dielectric spectroscopy. Aerosol particles are deposited in the form of a thin film on an electrode using electrostatic precipitation. Glass transition temperatures of glycerol and citric acid were measured, agreeing reasonably well with available literature data. By considering the intersect of super Arrhenius and Arrhenius lines, the new method appears to provide more reliable glass transition temperatures. The effect of cooling rates on glass transition temperatures were also investigated. I found that the measurements were conducted in a highly elegant way. The manuscript is clearly written and easy to follow. In fact, I enjoyed reading this manuscript very much.

My only major concern is that the method was validated with only two compounds. The authors plan to apply this method to measure glass transition temperatures of highly complex SOA mixtures in follow-up studies (L342). In this sense, it would be essential to test a few more compounds. There are indeed a number of organic compounds with known T_g, and I wonder why the authors would not have conducted some more measurements to consolidate this new method. Is this method too time-consuming or not so easy to be applied with more compounds?

We thank the reviewer for reading and reviewing our manuscript and his/her feedback. The reviewer brings up having more data to verify this technique, which we agree and did include more evidence. We would like to explain why we chose to use only glycerol in this study first. Glycerol is commonly used as a compound for characterizing and calibrating the performance of the dielectric spectroscopy. If the dielectric results of glycerol at all temperatures and all frequencies match previous literature, then the dielectric spectrometer is considered calibrated and all other compounds that have dielectric spectra should show similar results. As shown in Figure 3, the dielectric measurements of glycerol in our studies match the previous studies very well, showing that the dielectric spectrometer in our study is accurate and is able to give accurate results. We added Figure S1 to further prove that the derived relaxation timescales from our study also match the values from other literature at several different temperatures for glycerol.

We understand the reviewer's interest to see more results to validate the method. To include more evidence, we now show data for three other compounds besides glycerol and citric acid, and the results show very good agreement with the previous studies, not just for T_g measurement (as shown in Table 1, which could depend on the definition used), but also for the dielectric spectra at each temperature (Figure 5 in the main text and Figure S1 in the SI). The additional results further validate the results from our method. Please see the revised text, table, and figure below with additional data.

“As is shown in Table 1, the kinetically controlled glass transition data agree well with previously measured literature values of glycerol (Zondervan et al., 2007; Chen et al., 2012; Amann-Winkel et al., 2013), 1,2,6-hexanetriol (Nakanishi and Nozaki, 2010), di-n-butyl phthalate (Dufour et al., 1994), dioctyl phthalate (Beirnes Kimberley et al., 2003), and are within

3% of the literature value. The comparison of the dielectric relaxation timescale of glycerol measured from this study with literature values is shown in Figure S1, for several different temperatures. The results show that our measurements match the previously published results in the super-Arrhenius region when the compound is in equilibrium at a given temperature, with almost identical values.

Table 1. Glass transition temperatures for selected organic species at selected cooling or heating rates measured by broadband dielectric spectroscopy with a thin-film interdigitated electrode array

Compound	Chemical Formula	T _g (K)-Measured	T _g (K)-Literature
Glycerol	C ₃ H ₈ O ₃	<189 K (2 K/min)	190 K (Zondervan et al., 2007)
		192 ± 2 K (5 K/min)	191 K (Chen et al., 2012)
		194 ± 2 K (10 K/min)	196 K (Amann-Winkel et al., 2013) 191.7 ± 0.9 K (Lienhard et al., 2012)
1,2,6-hexanetriol	C ₆ H ₁₄ O ₃	192 ± 2 K (5 K/min)	196 K (Nakanishi and Nozaki, 2010)
di-n-butyl phthalate	C ₁₆ H ₂₂ O ₄	180 ± 2 K (5 K/min)	174 K (Dufour et al., 1994)
dioctyl phthalate	C ₂₄ H ₃₈ O ₄	194 ± 2 K (5 K/min)	190 K (Beirnes Kimberley and Burns Charles, 2003)
Citric Acid	C ₆ H ₈ O ₇	307 ± 5 K (5 K/min)	281 ± 5 K (Bodsworth et al., 2010)*
			285 ± 0.2 K (Lu and Zografis, 1997)
			281.9 ± 0.9 K (Lienhard et al., 2012)
			283-286 K (Dette et al., 2014)
			260 ± 10 K (Murray, 2008)**

* The data was based on modeling result. ** The data was based on fitting extrapolation result.

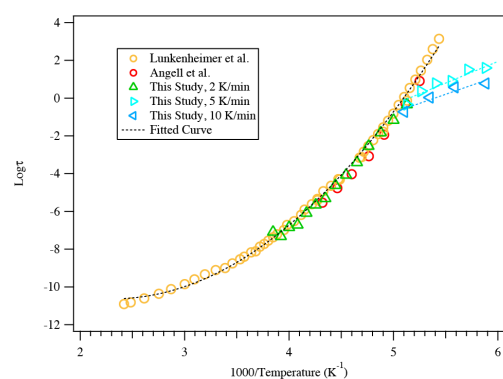


Figure S1. The logarithm of the relaxation timescale as a function of the inverse temperature derived from glycerol. The circles are from Lunkenheimer et al. (1999) and Angell (1995). The triangular points are experimental measurements from this work with different cooling rates. The dashed lines are the fitted curves for the super-Arrhenius and Arrhenius regions. The results show that the T_g values from this work match very well with previous studies.”

Minor comment: - L61: I suggest citing also Zobrist et al., PCCP, 13, 3514, 2011.

We thank the reviewer for the comment. Yes we agree this paper is very relevant and we have included the references that the reviewer provided.

- L72: Rothfuss and Petters, PCCP, 2017 measured the viscosity of sucrose but not various types of SOA (or did they?).

We thank the reviewer for the comment. The sentence has been changed to: “Rothfuss and Petters (2017) studied the viscosities of [sucrose particles with sodium dodecyl sulfate \(SDS\) particles](#) up to 10^7 Pa under sub-freezing temperature regimes.”

- L282: “the” should be replaced to “that”.

The word has been corrected.

- SI contains useful information (especially Figure S1 is interesting) and I suggest moving them into the main manuscript or appendix.

Thank you for the suggestion. We moved the Figure S1 to section 3.1 and named it Figure 6. We also added text to introduce Figure 6 as shown below.

“Our kinetically controlled dielectric spectra fitted using Eq. (S2) is shown in Figure 6. From the fitting results in Figure 6, the dielectric relaxation timescales τ are derived as a function of temperature, as shown in Figure 7.

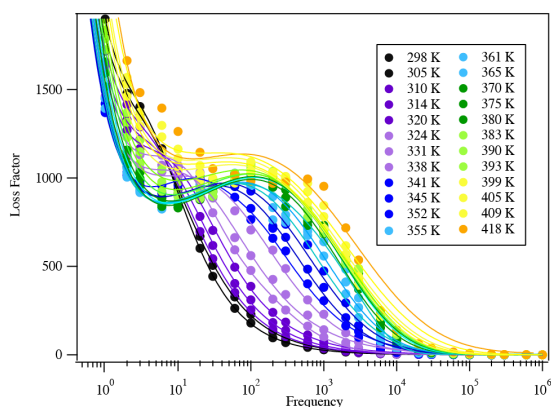


Figure 6. The dielectric relaxation spectrum of citric acid at different temperatures. The solid circles are measurement experimental data and the solid lines are fitting curves parameterized from Eq. (S2) and Adrjanowicz et al. (2009). ”

References

- Amann-Winkel, K., Gainaru, C., Handle, P. H., Seidl, M., Nelson, H., Böhmer, R., and Loerting, T.: Water's second glass transition, *Proc. Natl. Acad. Sci. USA*, 110, 17720-17725, 10.1073/pnas.1311718110, 2013.
- Angell, C. A.: Formation of glasses from liquids and biopolymers, *Science*, 267, 1924-1935, 1995.
- Angell, C. A.: Liquid Fragility and the Glass Transition in Water and Aqueous Solutions, *Chem. Rev.*, 102, 2627-2650, 10.1021/cr000689q, 2002.
- Bahous, H., Soufi, M. M., Meuret, L., and Benzohra, M.: Relaxation Time at Glass Transition Temperature Measured by Simplex Thermo Stimulated Depolarisation Current, *Macromolecular Symposia*, 341, 45-50, doi:10.1002/masy.201300158, 2014.
- Beirnes Kimberley, J., and Burns Charles, M.: Thermal analysis of the glass transition of plasticized poly(vinyl chloride), *J. Appl. Polym. Sci.*, 31, 2561-2567, 10.1002/app.1986.070310815, 2003.
- Bodsworth, A., Zobrist, B., and Bertram, A. K.: Inhibition of efflorescence in mixed organic-inorganic particles at temperatures less than 250 K, *Phys. Chem. Chem. Phys.*, 12, 12259-12266, 10.1039/C0CP00572J, 2010.
- Chen, Z., Sepúlveda, A., Ediger, M. D., and Richert, R.: Dielectric spectroscopy of thin films by dual-channel impedance measurements on differential interdigitated electrode arrays, *Eur. Phys. J. B*, 85, 1-5, 10.1140/epjb/e2012-30363-0, 2012.
- Detle, H. P., Qi, M., Schröder, D. C., Godt, A., and Koop, T.: Glass-Forming Properties of 3-Methylbutane-1,2,3-tricarboxylic Acid and Its Mixtures with Water and Pinonic Acid, *J. Phys. Chem. A*, 118, 7024-7033, 10.1021/jp505910w, 2014.
- Detle, H. P., and Koop, T.: Glass Formation Processes in Mixed Inorganic/Organic Aerosol Particles, *J. Phys. Chem. A*, 119, 4552-4561, 10.1021/jp5106967, 2015.
- Dufour, J., Jorat, L., Bondeau, A., Siblino, A., and Noyel, G.: Shear viscosity and dielectric relaxation time of dibutyl phthalate down to glass transition temperature, *J. Mol. Liq.*, 62, 75-82, [https://doi.org/10.1016/0167-7322\(94\)00764-0](https://doi.org/10.1016/0167-7322(94)00764-0), 1994.
- Elmatad, Y. S., Chandler, D., and Garrahan, J. P.: Corresponding States of Structural Glass Formers, *J. Phys. Chem. B*, 113, 5563-5567, 10.1021/jp810362g, 2009.
- Hudson, A.: *Statistical Mechanics and Dynamics of Liquids in and out of Equilibrium*, Ph.D., University of California, Berkeley, 2018.
- Keys, A. S., Garrahan, J. P., and Chandler, D.: Calorimetric glass transition explained by hierarchical dynamic facilitation, *Proc. Natl. Acad. Sci. USA*, 110, 4482-4487, 10.1073/pnas.1302665110, 2013.
- Kuwata, M., and Martin, S. T.: Phase of atmospheric secondary organic material affects its reactivity, *Proc. Natl. Acad. Sci. USA*, 109, 17354-17359, 10.1073/pnas.1209071109, 2012.

- Lienhard, D. M., Zobrist, B., Zuend, A., Krieger, U. K., and Peter, T.: Experimental evidence for excess entropy discontinuities in glass-forming solutions, *The Journal of Chemical Physics*, 136, 074515, 10.1063/1.3685902, 2012.
- Lienhard, D. M., Huisman, A. J., Bones, D. L., Te, Y.-F., Luo, B. P., Krieger, U. K., and Reid, J. P.: Retrieving the translational diffusion coefficient of water from experiments on single levitated aerosol droplets, *Phys. Chem. Chem. Phys.*, 16, 16677-16683, 10.1039/c4cp01939c, 2014.
- Limmer, D. T., and Chandler, D.: Theory of amorphous ices, *Proceedings of the National Academy of Sciences of the United States of America*, 111, 9413-9418, 10.1073/pnas.1407277111, 2014.
- Lu, Q., and Zograf, G.: Properties of citric acid at the glass transition, *J. Pharm. Sci.*, 86, 1374-1378, 10.1021/js970157y, 1997.
- Lunkenheimer, P., Schneider, U., Brand, R., and Loidl, A.: Broadband dielectric response of glycerol and propylene carbonate: a comparison, *AIP Conference Proceedings*, 469, 433-440, 10.1063/1.58527, 1999.
- Moynihan, C. T., Easteal, A. J., Wilder, J., and Tucker, J.: Dependence of the glass transition temperature on heating and cooling rate, *The Journal of Physical Chemistry*, 78, 2673-2677, 10.1021/j100619a008, 1974.
- Murray, B. J.: Inhibition of ice crystallisation in highly viscous aqueous organic acid droplets, *Atmos. Chem. Phys.*, 8, 5423-5433, 10.5194/acp-8-5423-2008, 2008.
- Nakanishi, M., and Nozaki, R.: Dynamics and structure of hydrogen-bonding glass formers: Comparison between hexanetriol and sugar alcohols based on dielectric relaxation, *Physical Review E*, 81, 041501, 2010.
- Saiter, J. M., Grenet, J., Dargent, E., Saiter, A., and Delbreilh, L.: Glass Transition Temperature and Value of the Relaxation Time at T_g in Vitreous Polymers, *Macromolecular Symposia*, 258, 152-161, doi:10.1002/masy.200751217, 2007.
- Shinyashiki, N., Shinohara, M., Iwata, Y., Goto, T., Oyama, M., Suzuki, S., Yamamoto, W., Yagihara, S., Inoue, T., Oyaizu, S., Yamamoto, S., Ngai, K. L., and Capaccioli, S.: The Glass Transition and Dielectric Secondary Relaxation of Fructose–Water Mixtures, *The Journal of Physical Chemistry B*, 112, 15470-15477, 10.1021/jp807038r, 2008.
- Shiraiwa, M., and Seinfeld, J. H.: Equilibration timescale of atmospheric secondary organic aerosol partitioning, *Geophys. Res. Lett.*, 39, L24801, 10.1029/2012GL054008, 2012.
- Simatos, D., Blond, G., Roudaut, G., Champion, D., Perez, J., and Faivre, A. L.: Influence of heating and cooling rates on the glass transition temperature and the fragility parameter of sorbitol and fructose as measured by DSC, *J. Therm. Anal.*, 47, 1419-1436, 10.1007/BF01992837, 1996.
- Zhang, Y., Chen, Y., Lambe, A. T., Olson, N. E., Lei, Z., Craig, R. L., Zhang, Z., Gold, A., Onasch, T. B., Jayne, J. T., Worsnop, D. R., Gaston, C. J., Thornton, J. A., Vizuete, W., Ault, A. P., and Surratt, J. D.: Effect of Aerosol-Phase State on Secondary Organic Aerosol Formation from the Reactive Uptake of Isoprene-Derived Epoxydiols (IEPOX), *Environ. Sci. Technol. Lett.*, 5, 167-174, 10.1021/acs.estlett.8b00044, 2018.
- Zondervan, R., Kulzer, F., Berkhout, G. C. G., and Orrit, M.: Local viscosity of supercooled glycerol near T_g probed by rotational diffusion of ensembles and single dye molecules, *Proc. Natl. Acad. Sci. USA*, 104, 12628-12633, 10.1073/pnas.0610521104, 2007.

1 **Kinetically Controlled Glass Transition Measurement of Organic Aerosol**
2 **Thin Films Using Broadband Dielectric Spectroscopy**

3
4 Yue Zhang^{1,2,£}, Shachi Katira³, Andrew Lee^{1,†}, Andrew T. Lambe², Timothy B. Onasch^{1,2}, Wen
5 Xu², William A. Brooks², Manjula R. Canagaratna², Andrew Freedman², John T. Jayne², Doug
6 R. Worsnop², Paul Davidovits^{1,*}, David Chandler^{3,§}, Charles E. Kolb^{2,*}

7
8 *1 Department of Chemistry, Boston College, Chestnut Hill, MA, 02459*

9 *2 Aerodyne Research Inc., Billerica, MA, 01821*

10 *3 Department of Chemistry, University of California, Berkeley, CA, 94720*

11 *£ Now at Department of Environmental Science and Engineering, Gillings School of*
12 *Global Public Health, University of North Carolina at Chapel Hill*

13 *† Now at Department of Chemistry, University of North Carolina at Chapel Hill*

14 *§Deceased April 2017*

15
16
17 April 2018

18
19 *Atmospheric Measurement Technology*

20
21 *Corresponding authors: Paul Davidovits, (617)552-3617, davidovi@bc.edu

22 Charles E. Kolb, (978)663-9500 x 290, kolb@aerodyne.com

23

24 **Abstract**

25 Glass transitions from liquid to semi-solid and solid phase states have important implications for
26 reactivity, growth, and cloud forming (cloud condensation nuclei and ice nucleation) capabilities
27 of secondary organic aerosols (SOA). The small size and relatively low mass concentration of
28 SOA in the atmosphere make it difficult to measure atmospheric SOA glass transitions using
29 conventional methods. To circumvent these difficulties, we have adapted a new technique for
30 measuring glass forming properties of atmospherically relevant organic aerosols. Aerosol
31 particles to be studied are deposited in the form of a thin film onto an interdigitated electrode
32 (IDE) using electrostatic precipitation. Dielectric spectroscopy provides dipole relaxation rates
33 for organic aerosols as a function of temperature (373 to 233K) that are used to calculate the
34 glass transition temperatures for several cooling or heating rates. IDE-enabled broadband
35 dielectric spectroscopy (BDS) was successfully used to measure the kinetically controlled glass
36 transition temperatures of aerosols consisting of [glycerol and four other compounds](#) with selected
37 cooling/heating rates. The glass transition results agree well with available literature data for
38 these [five compounds](#). The results indicate that the IDE-BDS method can provide accurate glass
39 transition data for organic aerosols under atmospheric conditions. The BDS data obtained with
40 the IDE-BDS technique can be used to characterize glass transitions for both simulated and
41 ambient organic aerosols and to model their climate effects.

42

43 **Keywords**

44 Broadband Dielectric Spectroscopy Glass Transition Organic Aerosols
45 Interdigitated Electrodes Thin Films Aerosol Climate Effects

46 **1 Introduction**

47 Aerosol particles have important climate and health effects because they can scatter
48 sunlight, form clouds by acting as cloud condensation nuclei (CCN), alter visibility, and affect
49 human health (Hallquist et al., 2009; Jimenez et al., 2009). Recent studies have confirmed that
50 organic aerosols, which comprise approximately half of the total submicron aerosol mass in the
51 atmosphere, can change from liquid to glassy state at ambient humidity levels and temperatures
52 (Zobrist et al., 2008; Virtanen et al., 2010; Shrestha et al., 2014; Zhang et al., 2015). The effect
53 of temperature may be especially important when aerosol particles are lifted into the free
54 troposphere, where the temperature change can rapidly alter their phase from liquid to glass
55 (Koop et al., 2011). The physical state of the aerosol strongly influences air quality and aerosol
56 climate effects. Evidence suggests that secondary organic aerosols, formed through oxidation of
57 gas phase organic compounds, have much lower vaporization rates than previously assumed,
58 which changes the reactivity of the gas phase species as well as their fate in the atmosphere. [The](#)
59 [phase state of aerosol particles also influences the diffusion of the gas phase species into the](#)
60 [atmosphere, affecting the oxidation extent and multiphase reactions of the particles. For](#)
61 [example, Shiraiwa and Seinfeld \(2012\) used models to predict that when aerosol particles are in](#)
62 [certain semi-solid and glassy phase states, the reactive uptake of gas phase species will be](#)
63 [kinetically limited. Kuwata and Martin \(2012\) showed that the phase state of secondary organic](#)
64 [aerosols \(SOA\) affects the uptake of ammonia into the particles. Zhang et al. \(2018\) provided](#)
65 [experimental and modeling evidence that the reactive uptake of isoprene-derived epoxydiols](#)
66 [\(IEPOX\) into acidic sulfate particles is influenced by the phase state, which can contribute to at](#)
67 [least a 30% reduction of isoprene-derived SOA in the Southeast U.S.](#)

68 [The phase state of the aerosols also affects their climate properties. For example, in the](#)

69 glassy state, the water vapor uptake by the SOA is greatly reduced, limiting the ability of
70 particles to [have liquid water condense on them](#) and thus hampering the formation of liquid
71 cloud droplets (Shiraiwa et al., 2011; Zobrist et al., 2011; Price et al., 2015). However, there is
72 evidence that glassy SOAs are effective ice nucleation agents. Their ability to nucleate ice
73 crystals to form Cirrus clouds in the upper troposphere may be particularly important given the
74 key role of these clouds in global warming (Wilson et al., 2012; Berkemeier et al., 2014). Lack
75 of adequate data describing these processes contributes to the high uncertainty of atmospheric
76 aerosol impact on climate change (Shiraiwa et al., 2017).

77 The importance of the phase state of organic aerosols in the evaluation of their climate
78 effects has motivated several studies in this field. However, these studies are difficult to perform
79 and the data obtained so far are limited. Renbaum-Wolff et al. (2013) studied the phase state and
80 viscosity of the water-soluble part of α -pinene SOA at several humidity levels and phase
81 separation effects. Zhang et al. (2015) characterized the viscosity of α -pinene SOA across a wide
82 range of relative humidity levels. Rothfuss and Petters (2017) studied the viscosities of [sucrose](#)
83 [particles with sodium dodecyl sulfate \(SDS\) particles](#) up to 10^7 Pa under sub-freezing
84 temperature regimes. There have also been a few studies exploring the glass transition
85 temperature of atmospherically relevant organic compounds by using differential scanning
86 calorimetry (DSC) (Koop et al., 2011; Lienhard et al., 2012; Dette et al., 2014; Dette and Koop,
87 2015).

88 Despite past studies, very little information is available on how organic aerosols become
89 glass as temperature, and the rate of cooling/heating changes. Such information is required to
90 model the aerosol phase when aerosols are transported from one region of the atmosphere to
91 another (Murray et al., 2010; Wilson et al., 2012). In an early 2011 study Koop and co-workers

92 performed experiments that led them to estimate glass transition temperature (T_g) values of 268-
93 290K for a range of surrogate biogenic SOA compounds by utilizing the DSC method. The
94 results show that oxidation and/or oligomerization reactions leading to higher oxygen to carbon
95 ratios (O:C) yield higher T_g values. Dette et al. (2014) used the “metastable aerosol by the low
96 temperature evaporation of solvent” (MARBLES) technique to provide information on the glass-
97 to liquid transition temperatures of pure organic compounds and organic-inorganic binary
98 mixtures. Their results show that the glass transition temperatures of these mixtures can be
99 accurately described by the Gordon-Taylor equation that describes the glass transition of binary
100 mixtures. However, to evaluate the impact of SOA and its possible phase transitions on climate
101 and air quality issues, the current techniques need to be improved in order to adapt to the
102 atmospheric aerosol sampling requirements.

103 The small particle size and relatively low concentration of SOA in the atmosphere make
104 it difficult to measure atmospheric SOA glass transitions using conventional methods. First, a
105 reliable measurement of glass transitions with currently used techniques requires a relatively
106 large mass, typically milligram levels of the compound, while reasonable field collection
107 methods yield organic aerosols in the femtogram mass range (Dette et al., 2014; Dette and Koop,
108 2015). Second, it is difficult to collect suspended aerosols and transfer them to the analysis
109 apparatus without contaminating the sample with trace water. Trace amounts of water absorbed
110 by SOA can substantially alter glass transition properties (Bateman et al., 2015; Price et al.,
111 2015; Rothfuss and Petters, 2017; Shiraiwa et al., 2017). To circumvent these difficulties, we
112 have adopted a new technique for measuring glass forming properties of atmospherically
113 relevant organic compounds. The technique combines broadband dielectric spectroscopy (BDS)
114 utilizing interdigitated electrodes (IDE) (Chen et al., 2012) with organic aerosol sample

115 deposition using electrostatic precipitation (Liu et al., 2013).

116 BDS is one of the most widely used techniques for measuring the dynamics and glass
117 transition of liquid and semi-solids (Richert, 2014). In the usual arrangement, dielectric
118 spectroscopy instruments consist of two parallel metallic plates with the sample filling the space
119 between the plates. As was stated, the traditional dielectric method usually requires mass in the
120 milligram range to perform the measurement (Richert, 2014). Such high mass loading cannot be
121 reasonably attained with aerosol collected under normal atmospheric conditions. A relatively
122 new technique, using interdigitated electrodes (IDE), which requires only one surface for
123 samples and requires mass only in the femtogram range (Chen et al., 2012), is suitable for
124 atmospheric aerosol phase studies. A thin film is deposited on the IDE first, then the dielectric
125 spectra are recorded to characterize the glass transition of aerosol particles at variable cooling or
126 heating rates.

127 The purpose of this study is to demonstrate the new IDE-BDS analysis technique by
128 presenting results of the glass transition of SOA surrogates using this technique. In section 2
129 below, we first describe the experimental setup including aerosol generation, thin film deposition
130 on the IDE, temperature conditioning chamber, and the BDS measurement system. Then data
131 analysis, including glass transition determination, is discussed in section 3. Section 4 includes
132 discussion of the advantages of the IDE-BDS method, as well as caveats associated with its
133 current implementation.

134 **2. Experimental Setup**

135 A schematic diagram of the experimental setup is shown in Figure 1. The setup is
136 conveniently divided into four parts: 1. Aerosol sample generation, 2. Thin film formation via
137 electrostatic precipitation on the Interdigitated electrodes (IDE) with associated humidity control

138 3. Temperature conditioning chamber and 4. Broadband Dielectric Spectroscopy measurement
139 system.

140 **2.1 Aerosol generation.**

141 Two types of aerosol generation systems are used in our experiments. The first is a home-
142 made self-nucleation generation device used for producing liquid organic aerosol samples
143 including glycerol, 1,2,6-hexanetriol, di-n-butyl phthalate, and dioctyl phthalate. About 0.5 gram
144 of the glycerol is placed at the bottom of a round flask and the temperature of the flask is heated
145 to 20°C below the boiling temperature of the organic liquid. A condenser is connected to the top
146 of the flask to cool the temperature of that region. A flow of 2 liters per minute (Lpm) of dry air
147 passes through the condenser and brings the aerosol particles to the region where the aerosols are
148 precipitated onto the IDE.

149 The second method utilizes a commercial unit (TSI, 3076) to generate atomized citric
150 acid aerosols. About 0.5 gram of citric acid is dissolved in 100 mL of high purity water to form
151 the atomizing solution. About 30 psi pressure of dry air is applied on one end of the atomizer to
152 generate a constant 3 Lpm aerosol-containing flow to the second part of the system, which is the
153 thin film generation system that will be described below.

154 **2.2 Interdigitated electrode (IDE) and thin film formation.**

155 An IDE (NIB003744, MS-01/60, NETZSCH Instrument North America) is used in this
156 study as a substrate for measuring the dielectric constants of organic materials. The IDE consists
157 of two thin electrodes that are interdigitated together like entwined finger tips, as shown in
158 Figure 2. Each interdigitated pair serves as a small capacitor for dielectric analysis. The thin
159 electrodes are made from platinum (Pt) and are arrayed on a quartz substrate. The electrodes
160 utilized in this study are spaced 1 μm apart and are able to withstand temperatures up to 200 °C.

161 The combination of multiple interdigitated pairs of electrodes greatly enhances the sensitivity of
162 the technique compared to a single pair of electrodes that would have been used in the
163 conventional technique.

164 An electrostatic deposition method is used to deposit organic films on the IDE (Liu et al.,
165 2013). The electrostatic precipitator has one inlet and one outlet. A stream of aerosolized
166 oxygenated organic liquid droplets to be studied is passed through an inlet with a high voltage
167 corona discharger (-5000V) so that all the droplets are negatively charged to varying degrees. The
168 flow is directed above the substrate held at +3000 V within the precipitator. Due to opposite
169 charges, the charged particles are electrostatically deposited onto the substrate, gradually merging
170 together to form thin films. The remaining flow is then withdrawn from the precipitator and flows
171 through a HEPA filter connected to a pump. The flow rate through the precipitator is maintained
172 between 1.7-1.9 Lpm. Depending on the amount of aerosol material being deposited onto the
173 surface, the deposition can remain either remain as discrete aerosol droplets, or at higher droplet
174 depositions, can form a uniform thin film, as shown in Figure 2. For this study thin films are
175 formed. The volume concentration of the aerosol particles at the inlet of the precipitator was
176 $4.5 \times 10^{11} \text{ nm}^3 \text{ cm}^{-3}$. After collecting for 5 hours, the film thickness is estimated to be 1-2 μm on a
177 $1 \text{ mm} \times 8 \text{ mm}$ substrate based on the difference of volume concentration between the inlet and the
178 outlets of the precipitator, the flow rate, the collection time, and assuming 50% collection
179 efficiency.

180 **2.3 Temperature conditioning chamber.**

181 The IDE substrate coated with organic material is then transported to the temperature
182 conditioning chamber using tweezers. The temperature conditioning chamber consists of a
183 stainless steel cap and a heating/cooling surface using either a liquid nitrogen cooler or a heating

184 furnace. The sample temperature can be controlled from \sim -150°C to +200°C. Details of the
185 chamber are shown in Figure 1. The cooling/heating rate can be varied from 1 K/min to 25
186 K/min. The chamber is flushed with dry nitrogen gas to reduce the relative humidity (RH) prior
187 to temperature conditioning. A K type thermocouple is located on top of a reference cell inside
188 the conditioning chamber, to monitor sample temperature. The typical cooling cycle starts
189 around 20 °C and ends at about -140 °C, while the heating cycle starts at -140 °C and ends at 30
190 °C. The cooling and heating cycle are adjusted to the desired cooling/heating rates between 2
191 K/min and 10 K/min.

192 **2.4 Broadband Dielectric Spectroscopy (BDS) measurement system.**

193 The BDS instrument used in this study is manufactured by NETZSCH Inc. (DEA 288
194 model). A periodic signal from the instrument is applied to the IDE electrodes. The frequency of
195 the signal ranges from 10^{-3} Hz to 1 MHz. The data acquisition part of the instrument then
196 measures the impedance, Z_{sample} , of the sample as a function of the applied frequency. The
197 impedance measurement yields the capacitance of the sample on top of the IDE. By measuring
198 the impedance of the uncoated and organic-coated IDE, three IDE capacitances can be obtained,
199 i.e., when the IDE is uncoated, Z_{empty} , when it is coated with organic compounds, Z_{coated} , and the
200 geometric capacitance of the IDE without any substrate, Z_{geo} . Approximate values of the real and
201 imaginary part of the sample permittivity, ϵ_{sample} , can be obtained using Eq. (1) (Chen et al.,
202 2012)

$$203 \quad \epsilon_{\text{sample}} = 1 + \frac{Z_{\text{loaded}} - Z_{\text{empty}}}{Z_{\text{geo}}} \quad (1)$$

204 For demonstration and data comparison purposes, we have used glycerol, [1,2,6-](#)
205 [hexanetriol](#), [di-n-butyl phthalate](#), and [dioctyl phthalate](#) (99%, Sigma Aldrich, St. Louis, MO,
206 USA) as the test compounds for homogeneous nucleation and citric acid (99%, Sigma Aldrich,

207 St. Louis, MO, USA) as the surrogate organic aerosol generated by atomizing solutions. For
208 atomizing solutions, the surrogate compound is mixed with high purity water. All reagents were
209 used as provided without further purification.

210 3. Data Analysis

211 3.1 Calculating Relaxation Time τ

212 The thin film on the IDE is usually cooled at a selected cooling rate and then heated back to 30°C.
213 After a cooling-heating cycle, the dielectric constant at each temperature measured, $\varepsilon(\omega)$, is
214 recorded by instrument. The relaxation time, τ , can be obtained by curve fitting the Havriliak-
215 Negami equation of the real and imaginary parts ($\varepsilon'(\omega)$ and $\varepsilon''(\omega)$), respectively) with the
216 frequency ω , as shown in Figure 3 (Chen et al., 2012). The detailed equation for $\varepsilon'(\omega)$ and $\varepsilon''(\omega)$
217 is shown in Eqns. (S1) and (2). At each temperature, the dielectric spectra often show peaks at
218 specific frequencies, designated as dielectric relaxation peaks. Different peaks give different τ
219 values after fitting Eq. (2) with the data points.

$$220 \quad \varepsilon''(\omega) = \Delta\varepsilon(1 + 2(\omega\tau)^\alpha \cos\left(\frac{\pi\alpha}{2}\right) + (\omega\tau)^{2\alpha})^{-\beta/2} \sin(\beta\varphi) \quad (2)$$

$$221 \quad \text{with } \Delta\varepsilon = \varepsilon_s - \varepsilon_\infty, \quad \varphi = \arctan\left(\frac{(\omega\tau)^\alpha \sin\left(\frac{\pi\alpha}{2}\right)}{1 + (\omega\tau)^\alpha \cos\left(\frac{\pi\alpha}{2}\right)}\right)$$

222 where ε_s is the permittivity at lower frequency, ε_∞ is the permittivity at the high frequency limit,
223 α, β are fitting parameters, and τ is the characteristic relaxation time of the medium
224 (Adrjanowicz et al., 2009; Chen et al., 2012).

225 $\text{Log } \tau$ is then plotted as a function of the inverse of the temperature to further examine
226 how relaxation time changes as a function of temperature. The error bar represents twice the
227 standard deviation of the fitting result. The resulting curve can be used to calculate the glass
228 transition temperature of the compound, as described in section 3.2.

229 3.2 Glass Transition Determination

230 The glass transition temperature is defined as the temperature where a compound changes
231 from liquid to glass. Several methods have been used to indirectly determine the glass transition
232 temperatures. A common way to calculate the glass transition temperature using BDS is to measure
233 relevant parameters and to calculate the dielectric relaxation τ described in section 3.1 at several
234 equilibrium temperatures T , and then plot $\log \tau$ as a function of $1000/T$. The data points are fitted
235 using the Vogel-Fulcher-Tammann (VFT) formula (Vogel, 1921; Fulcher, 1925; Tammann and
236 Hesse, 1926). The glass transition is customarily defined as the temperature where $\tau=100$ s in the
237 fitted curve (Chen et al., 2012; Richert, 2014). The result usually agrees with the DSC
238 measurement within a few degrees (Richert, 2014). However the method is limited, because not
239 all compounds become glass as $\tau=100$ s (Saiter et al., 2007; Bahous et al., 2014). Furthermore, this
240 method does not take into account kinetic effects on glass transition, specifically the effect of
241 cooling and heating rates (Elmatad et al., 2009, 2010; Keys et al., 2013; Limmer and Chandler,
242 2014; Hudson and Mandadapu, 2018), as glass transition temperature changes with cooling and
243 heating rates.

244 The method used in our studies is based on dynamical facilitation theory (Elmatad et al.,
245 2009; Chandler and Garrahan, 2010; Keys et al., 2011; Keys et al., 2013; Hudson, 2015, Hudson
246 and Mandadapu, 2018), which also takes into account the effect of cooling rate on the glass
247 transition. According to this theory, as a compound is cooled and transitions from a liquid to a
248 supercooled liquid it exhibits super-Arrhenius behavior given by the following equation:

$$249 \log \tau/\tau_0 = J^2(1/T - 1/T_0)^2 \quad (3)$$

250 where J is an energy scale intrinsic to each material related to the rate of motion of
251 individual molecules, T_0 is termed the “onset temperature” and refers to the temperature at which

252 a liquid showing Arrhenius relaxation becomes a supercooled liquid showing super-Arrhenius
253 relaxation, and τ_0 is a temperature-independent reference time scale of the order of the time taken
254 for molecules to locally rearrange (Keys et al., 2011).

255 As temperature further decreases, the supercooled liquid becomes glass-like, exhibiting
256 Arrhenius behavior. The temperature where the supercooled liquid changes to glass is the glass
257 transition temperature of the compound at the specific cooling rate studied. As the sample is
258 continuously cooled at a specific cooling rate, the dielectric relaxation peaks can be generated as
259 a function of the sample temperature. The experimentally obtained data are plotted in the form
260 $\log \tau$ vs $1/T$. The data obtained at the higher temperature range are fitted to the super-Arrhenius
261 function and the data obtained at the lower temperature range are fitted to the Arrhenius function.
262 Figure 4 shows a typical relationship between the dielectric relaxation timescale and the
263 temperature, as a compound is cooled down or warmed up between the liquid state and glassy
264 state. As illustrated in Figure 4, the kinetically controlled glass transition temperature (or the true
265 glass transition temperature) is the temperature at the intersection of the two functions. The
266 traditional method determines the glass transition temperature as shown in dashed lines where τ
267 $=100$ s. Depending on the compound, the true glass transition temperature may not be the same
268 as the glass transition temperature determined by using $\tau=100$ s, as shown in section 4 below.
269 The uncertainty of the glass transition temperature is estimated based on varying the fitting
270 parameters of the super-Arrhenius curve and Arrhenius line within a one-sigma range.

271 For glycerol, measurements of glass transitions were performed at three cooling rates: 2
272 K/min, 5 K/min, and 10 K/min. At each cooling rate the compound is cooled from approximately
273 300 K to 125 K, while the dielectric peaks are measured simultaneously as a function of
274 temperature. The organic film is thin enough so that its temperature reaches equilibrium with the

275 cooling/heating medium, reducing the errors caused by heat transfer within the sample itself.
276 Such measurements are difficult to perform with conventional techniques due to slow heat
277 transfer in large mass samples, which often leads to inaccurate results. The effect of cooling rates
278 on glass transition measurements will be discussed in the following section.

279 **4 Results and Discussion**

280 **4.1 Glass transition temperature of selected organic compounds**

281 Aerosols are generated by two methods in this study, and in each method, we measured
282 the glass transition of a compound that has been studied in the literature. Glycerol, 1,2,6-
283 hexanetriol, di-n-butyl phthalate, dioctyl phthalate, and citric acid particles were generated
284 through the homogeneous nucleation method or the atomizer method, respectively. The
285 measured dielectric spectra of each compound show distinct relationships of their dielectric
286 relaxation timescales with a 5 K/min cooling rate, as shown in Figure 5. This is a confirmation of
287 the expected behavior.

288 By calculating the corresponding temperature when the super-Arrhenius curve intersects
289 with the Arrhenius curve, the glass transition of each compound can be derived. As is shown in
290 Table 1, the kinetically controlled glass transition data agree well with previously measured
291 literature values of glycerol (Zondervan et al., 2007; Chen et al., 2012; Amann-Winkel et al.,
292 2013), 1,2,6-hexanetriol (Nakanishi and Nozaki, 2010), di-n-butyl phthalate (Dufour et al.,
293 1994), dioctyl phthalate (Beirnes Kimberley et al., 2003), and measured values are within 3% of
294 the cited literature value. The comparison of the dielectric relaxation timescale of glycerol
295 measured in this study with literature values is shown in Figure S1, for several different
296 temperatures. The results show that our measurements match the previously published results in
297 the super-Arrhenius region when the compound is in equilibrium at a given temperature, with

298 almost identical values. As the temperature continues to drop, glycerol and other compounds we
299 tested fall out of equilibrium and become glass, which exhibits Arrhenius behavior. The
300 transition from super-Arrhenius to Arrhenius behavior in this study provides the kinetically
301 controlled glass transition as the compounds change from liquid to glassy state.

302 For citric acid, there is no dielectric measurement available. The kinetically controlled
303 dielectric spectra fitted using Eq. (S2) are shown in Figure 6. From the fitting results in Figure 6,
304 the dielectric relaxation timescales τ are derived as a function of temperature, as shown in Figure
305 7. The kinetically controlled glass transition temperature derived from Figure 7 agrees
306 reasonably well (within 10% error) with four literature results (Lu and Zografi, 1997; Bodsworth
307 et al., 2010; Dette et al., 2014; Lienhard et al., 2014). The fifth set of literature data (Murray,
308 2008) is based on extrapolation of a fit to experimental data and is about 20K lower than other
309 values reported by the literature. The differences can be explained by the following reasons: (1)
310 To date there have been no measurements of the dielectric spectra for citric acid to our
311 knowledge. The citric acid references in Table 1 are based on DSC measurements, which may
312 not be in exact agreement with the dielectric measurement. Angell (2012) pointed out that there
313 are at least three different definitions of the glass transition and the T_g determined by each can
314 be 50 K different from each other. DSC uses heat capacity changes to measure the glass
315 transition while dielectric relaxation uses molecular movements to define the glass transition.
316 Due to the difference in measurement parameters and the definition of the glass transition, these
317 two measurements can provide different T_g values of the same compound by up to 10 K
318 (Shinyashiki et al., 2008). (2) This study focuses on the kinetically controlled glass transition
319 temperature at a given cooling rate, i.e., the transition between the Arrhenius and super-
320 Arrhenius relaxation regimes to determine the glass transition temperature. If the more

321 conventional method, i.e. fitting the super-Arrhenius curve to obtain the glass transition
322 temperature when $\tau=100$ s, is applied to the data, as shown in Figure 7, the obtained glass
323 transition temperature would be 281 ± 3 K, which is within 1% difference compared with the
324 two nearest literature values. However, as previous publications have pointed out (Keys et al.,
325 2013; Bahous et al., 2014; Limmer and Chandler, 2014; Hudson, 2018), using the transition from
326 super-Arrhenius to Arrhenius region is likely to reflect the true glass transition when taking
327 kinetic factors, such as cooling/heating rates, into consideration. (3) Moreover, glass transition
328 data of citric acid are rather limited and there are differences between each study. For instance,
329 from the literature data, the differences between three reported glass transition temperatures are
330 up to 10%, which is about the same difference obtained by comparing our data to the other two
331 nearest literature results. (4) The heating and cooling rates may also contribute to the difference
332 of the T_g of citric acid between the literature and this study, as this study uses a lower cooling
333 rate than the ones reported by the literature. Moynihan et al. (1974) reported that a change of 2
334 K/min to 10 K/min cooling rate could alter the glass transition temperature of borosilicate by 15
335 K. It is possible that citric acid is a less fragile liquid, similar to borosilicate, i.e., the glass
336 transition temperature depends strongly on cooling or heating rates. Therefore, the difference
337 herein is likely due to including kinetic considerations such as heating/cooling rates in the
338 measurement of the glass transition. We report the citric acid glass transition temperature as 307
339 ± 5 K at 5 K/min warming rate, which is likely a more accurate way of reflecting the glass
340 transition, as the kinetic process is considered, as shown in Figure 7.

341 Even though the issues listed above are likely to be the primary reasons leading to ~10%
342 difference of the glass transition temperature of citric acid between our results and the literature,
343 the following factors may play a role: (1) Atomizing the citric acid solution and re-depositing

344 citric acid particles via electrostatic precipitation could introduce impurities during the
345 atomization process [that](#) may affect the glass transition temperatures; (2) The glass transition of
346 citric acid was measured during a warming cycle. A fast non-recordable cooling cycle at
347 20K/min was performed prior to warming in order to inhibit the citric acid crystal formation. The
348 hysteresis effect will lead to an increase of the glass transition temperature from the warming
349 cycle compared with data obtained from the cooling cycle (Wang et al., 2011); (3) Lu and
350 Zografi (1997) have shown that different ways of preparing the citric acid can lead to differences
351 in glass transition measurements. The thicknesses of the thin films are equal to or less than one
352 micrometer, leading to confinement effects and differences in glass transition temperature
353 measured from bulk compounds (Park and McKenna, 2000). The results show that the thin film
354 IDE-BDS method can accurately measure the glass transition temperatures of various organic
355 compounds that are comparable to the composition of organic aerosols.

356 **4.2 The influence of cooling rates on glass transition temperatures**

357 One advantage of this study is the introduction of cooling and heating rates as variables for
358 glass transition temperature measurement for organic compounds. For BDS studies, the glass
359 transition temperature of a compound is often deduced by measuring the sample at a few
360 isothermal temperatures and fitting the curve of temperature and relaxation time in order to identify
361 the temperature when relaxation time corresponds to 100 s. This traditional approach makes it
362 difficult to directly compare the result with glass transition temperatures deduced from DSC
363 studies with variable cooling rates. One of the advantages of our technique is that variable cooling
364 rate measurements are performed on the thin film and the cooling rate dependent glass transition
365 temperature of target species is determined.

366 The influence of cooling rate on glass transition temperature was carefully examined by
367 repeating the glycerol experiment at two additional cooling rates. The resulting super-Arrhenius
368 curve for each cooling rate is plotted against the Arrhenius lines of that cooling rate, as shown in
369 Figure 8. As a compound remains in the supercooled liquid stage, the relaxation time is short
370 enough that it is constantly in equilibrium with external perturbations, leading the super-Arrhenius
371 region totally reversible so it should behave the same for all cooling rates. The super Arrhenius
372 part of the data from all three different cooling rates all collapse into one single trend, indicating
373 the data collected agree well with the theory. The super-Arrhenius curve in Equation (3) from
374 Elmatad et al. (2009) is also plotted as the black dashed line and it also agrees well with our
375 experimental results. As the cooling continues, the relaxation time gets longer until it cannot keep
376 up with the external temperature change, leading to the compound falling out equilibrium and
377 forming a glass. Therefore, a faster cooling rate often leads to a quick falling out of equilibrium
378 and a higher glass transition temperature for the compounds studied, as demonstrated in Figure 8.
379 Based on the intercept of the super-Arrhenius curve and the Arrhenius line, the glass transition
380 temperatures for 5 K/min and 10 K/min cooling are determined to be 192 ± 2 K and 194 ± 2 K.
381 For 2 K/min cooling, because an Arrhenius line does not appear within our range of measurement,
382 the glass transition temperature will likely be lower than 189 K. This study reports an increase of
383 5 K or more in the glass transition of glycerol as the cooling rate changes from 2 K/min to 10
384 K/min. The reported increase in glass transition temperature during these cooling rates agrees with
385 the behavior of sorbitol and fructose in another study performed by Simatos et al. (1996), which
386 also measured the dependence of glass transition temperature on cooling rate with small organic
387 molecules.

388 Our results agree reasonably well with other studies for the glass transition temperatures
389 of [the five compounds chosen](#). However, there are a couple possible caveats for this study. One
390 is the influence of humidity during the cooling process. Even though dry nitrogen is used to flush
391 through the cooling chamber to remove any extra water vapor present prior to cooling, there is still
392 the possibility that the chamber wall surface can degas and release water vapor to the system during
393 the cooling process. The effect of water vapor on the testing materials is likely to be small, but
394 should be considered when the organic compound tested can readily absorb water at low RH
395 conditions. The other potential caveat is the influence of non-equilibrium heat transfer within the
396 thin film on the measurement of the glass transition temperature. Because the sample is being
397 cooled from underneath, the heat transfer between the upper and lower boundaries of the film can
398 lead to uncertainties in measuring the glass transition temperature. The organic thin films made
399 during the experiments are within the micrometer range, therefore the thermal gradient [across the](#)
400 [film](#) is small enough to be likely insignificant compared with other systematic errors. Moreover,
401 theoretical models to predict the glass transition of compounds with variable cooling rates are
402 needed in further studies to verify and explain these experimental measurements.

403 **5 Summary**

404 In this work, we have demonstrated a novel method using interdigitated electrodes,
405 broadband dielectric spectroscopy, and electrostatic precipitation together as an efficient and
406 powerful approach studying the phase and glass transitions of organic particles under various
407 cooling rates. The method is particularly suitable for studying the glass transition of submicron
408 organic particles whose mass loading is generally too small for other kinds of glass transition
409 measurement techniques. The results from this technique agree well with published studies using

410 other methods. Future publications will report glass transition measurements for simulated SOA
411 mixtures as well as laboratory produced SOA particles.

412 The dielectric relaxation peaks of [glycerol and four other compounds](#) were recorded, and
413 the logarithm of characteristic relaxation time were calculated and plotted as a function of inverse
414 temperature. The transition between the super-Arrhenius and Arrhenius curves were used to
415 determine the temperature where the super-cooled liquid fell out of equilibrium to become glass,
416 which is defined as the true experimental glass transition temperature. Furthermore, cooling rates
417 are demonstrated to have an effect on the glass transition temperature. By changing the cooling
418 rate from 2 K/min to 10 K/min, the glass transition temperature increases by at least 5 K for
419 glycerol.

420 **Acknowledgments** We acknowledge James Brogan, Yatish Parmar, Leonid Nichman, Professor
421 Ranko Richert, Lindsay Renbaum-Wolff, Wade Robinson, Paul Keabian, Professor Jason D.
422 Surratt, and Professor Andrew Ault for useful discussions and assistance with the experiments.

423 **Funding** This material is based upon work supported by the National Science Foundation
424 Environmental Chemistry Program in the Division of Chemistry under Grant No. 1506768, No.
425 1507673, and No. 1507642.

426 **Competing financial interests:** The authors declare no competing financial interests.

Table 1. Glass transition temperatures for selected organic species measured by broadband dielectric spectroscopy with a thin-film interdigitated electrode array

Compound	Chemical Formula	T _g (K)-Measured	T _g (K)-Literature
Glycerol	C ₃ H ₈ O ₃	<189 K (2 K/min)	190 K (Zondervan et al., 2007)
		192 ± 2 K (5 K/min)	191 K (Chen et al., 2012)
		194 ± 2 K (10 K/min)	196 K (Amann-Winkel et al., 2013) 191.7 ± 0.9 K (Lienhard et al., 2012)
1,2,6-Hexanetriol	C ₆ H ₁₄ O ₃	192 ± 2 K (5 K/min)	196 K (Nakanishi and Nozaki, 2010)
Di-n-butyl Phthalate	C ₁₆ H ₂₂ O ₄	180 ± 2 K (5 K/min)	174 K (Dufour et al., 1994)
Dioctyl Phthalate	C ₂₄ H ₃₈ O ₄	194 ± 2 K (5 K/min)	190 K (Beirnes Kimberley et al., 2003)
Citric Acid	C ₆ H ₈ O ₇	307 ± 5 K (5 K/min)	281 ± 5 K (Bodsworth et al., 2010)*
			285 ± 0.2 K (Lu and Zografis, 1997)
			281.9 ± 0.9 K (Lienhard et al., 2012)
			283-286 K (Dette et al., 2014)
			260 ± 10 K (Murray, 2008)**

* The data was based on modeling result. **The data was based on extrapolation of a fit to the data..

List of Figures

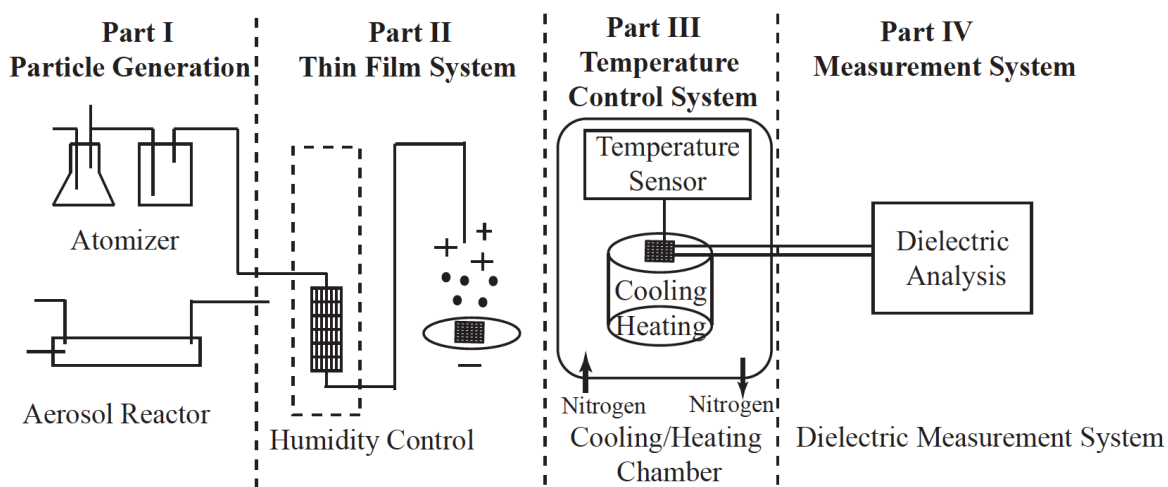


Figure 1. A schematic diagram of the experimental setup and procedure. The experimental approach consists of four parts: aerosol generation, thin film deposition using an electrostatic precipitator, the temperature control system, and the broadband dielectric spectroscopy measurement system.

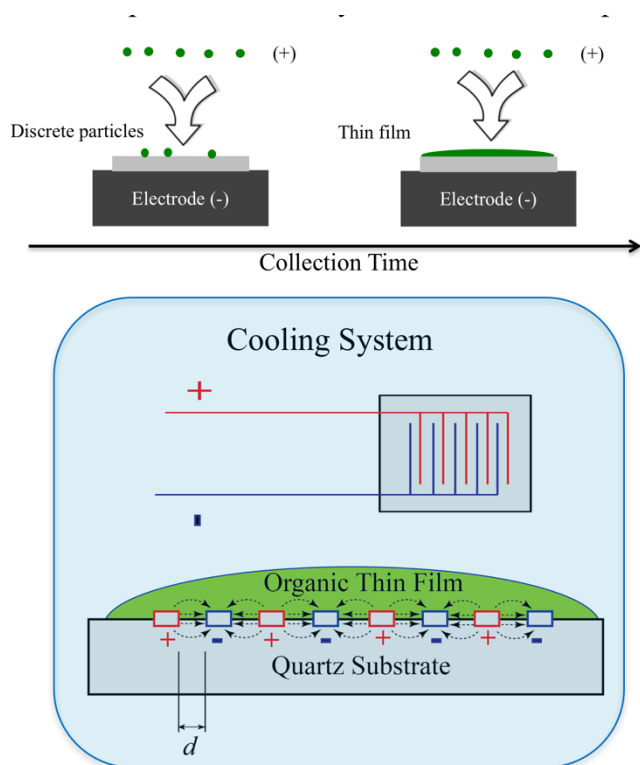


Figure 2. A schematic diagram of the key experimental setup. The upper panel shows the formation of organic thin films through electrostatic deposition. The lower panel shows the working principle of broadband dielectric spectroscopy (BDS) with an interdigitated electrode sensor. A compound is placed on an array of interdigitated electrodes with a periodic voltage, and the compound's impedance is recorded.

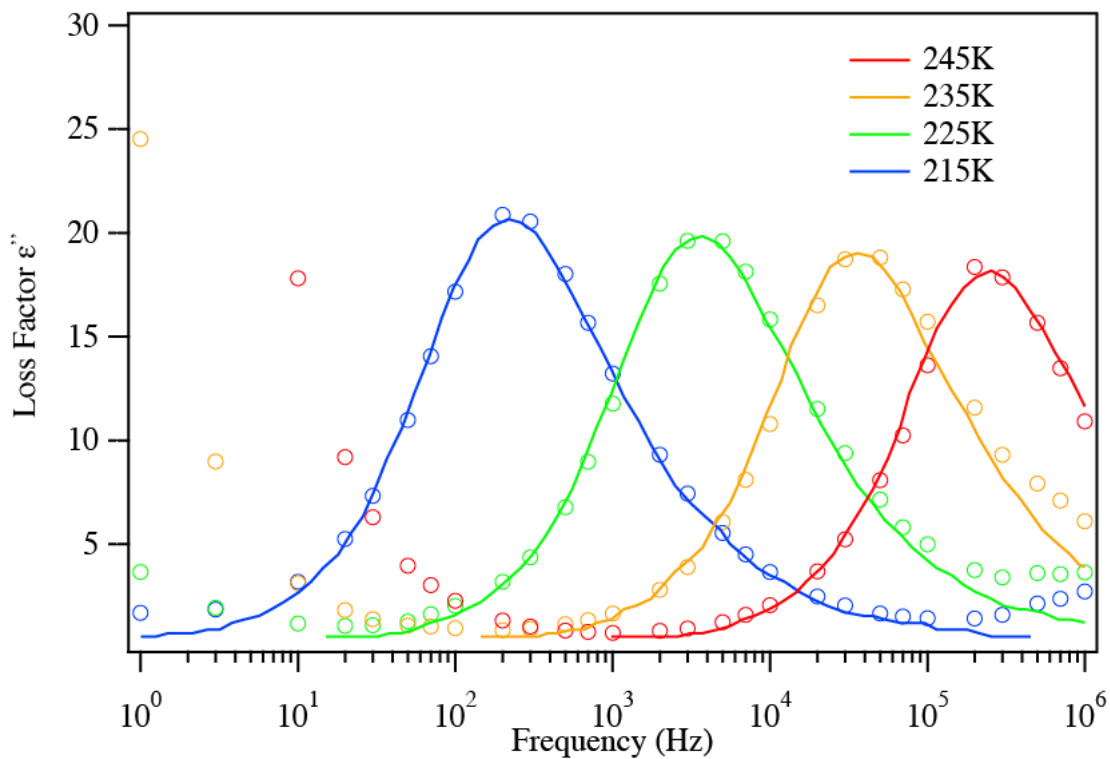


Figure 3. The dielectric relaxation spectrum of glycerol at different temperatures. The open circles are measured experimental data and the solid lines are literature data from Chen et al. (2012). As temperature decreases, the dielectric peaks shift towards lower frequencies, indicating that the relaxation timescale increases.

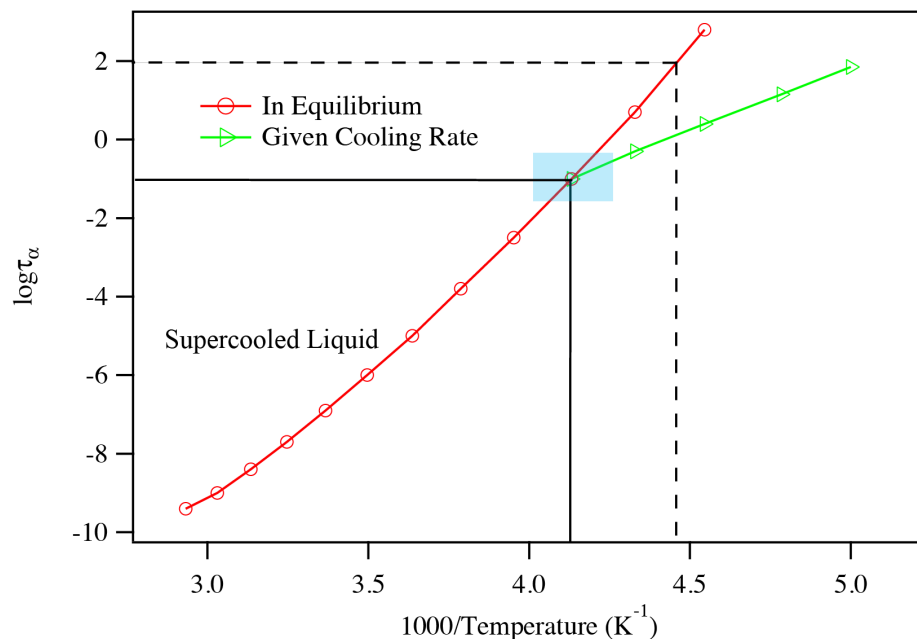


Figure 4. An illustrated plot of the relationship between dielectric relaxation time scale and temperature. The logarithm of the relaxation is plotted against inverse T, i.e., $\log \tau$ vs $1000/T$. By linking the data points together, one can plot the super-Arrhenius curve (red) and the Arrhenius line (green). Using a consistent cooling rate, the intersection of the two regions identifies the compound's glass transition temperature, as indicated by the shaded blue region. The intersection of the two black lines represents the glass transition point. The intersection of the two black dashed lines shows the glass transition temperature determined using the traditional method of identifying the temperature when $\tau=100$ s.

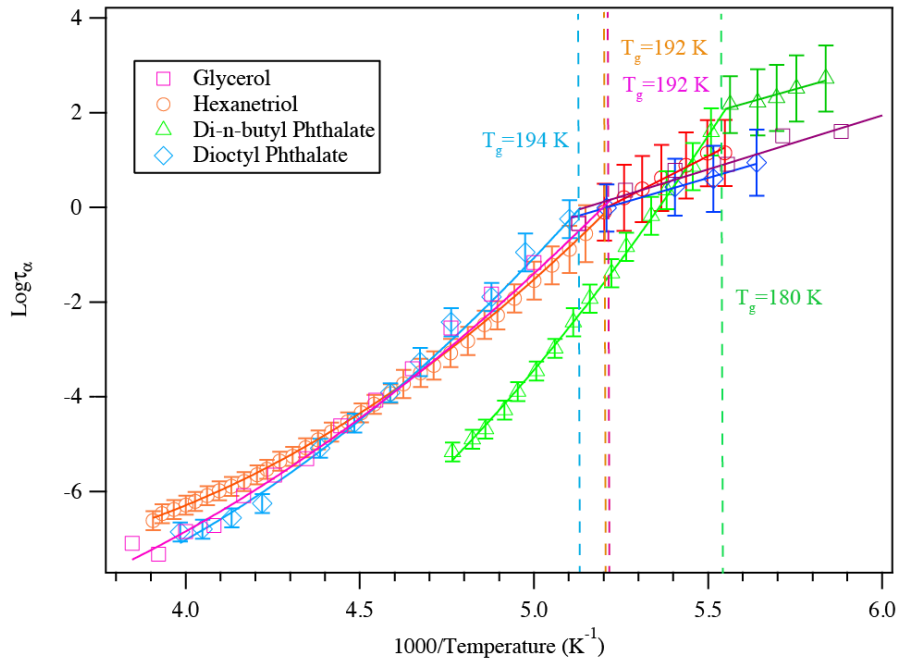


Figure 5. A plot of superimposed data points and curves constructed for glycerol, 1,2,6-hexanetriol, di-n-butyl phthalate, and dioctyl phthalate cooled at 5K/min. The solid color lines represent the fitted curves for the super-Arrhenius and Arrhenius region. The intersection between the two lines indicates the kinetically controlled glass transition region for each compound. The glass transition at a 5K/min cooling rate for each compound is shown in the plot.

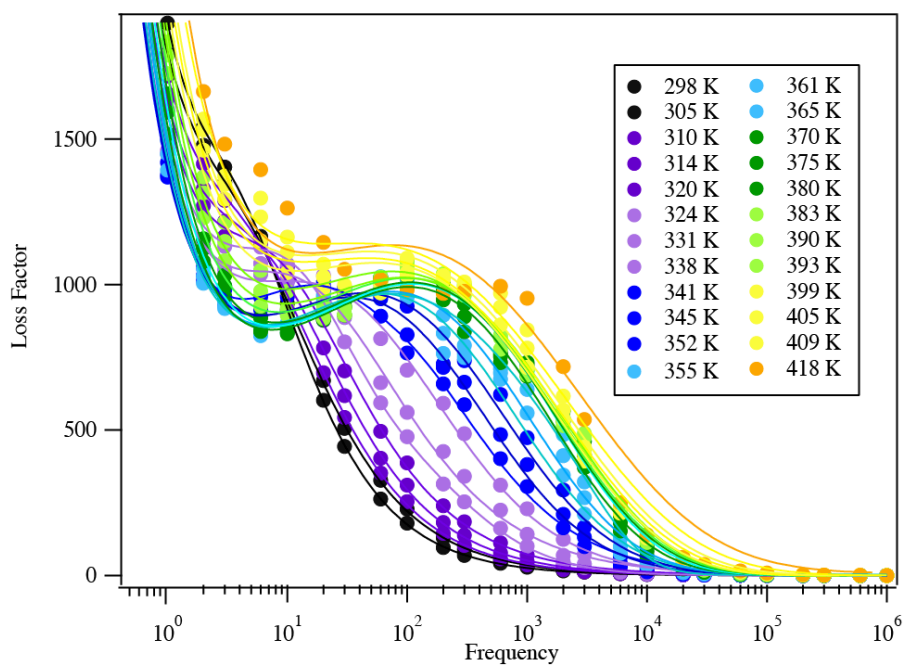


Figure 6. The dielectric relaxation spectrum of citric acid at different temperatures. The solid circles are measured experimental data and the solid lines are fitted curves parameterized from Eq. (S2) and Adrjanowicz et al. (2009).

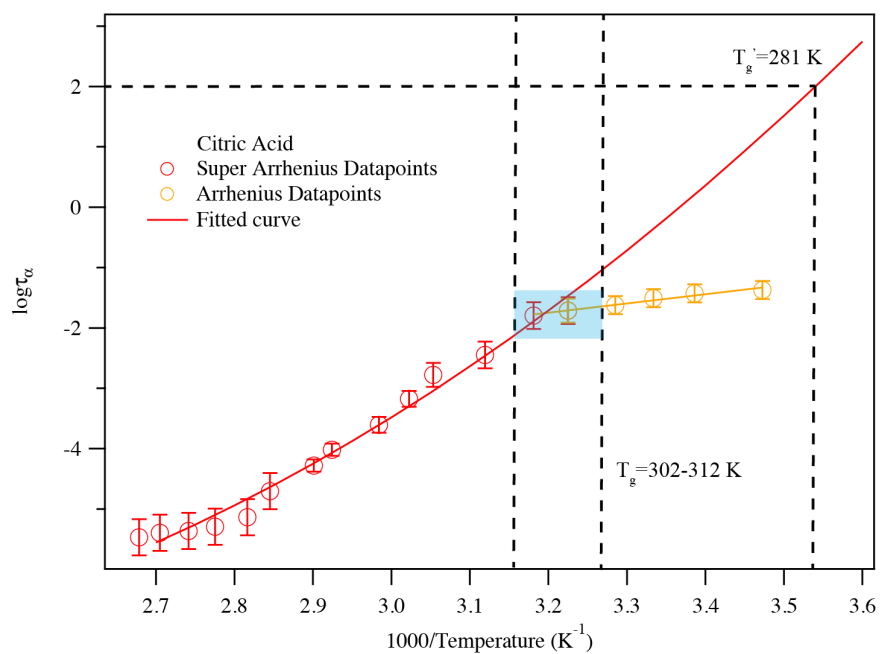


Figure 7. A plot of superimposed data-points and curves constructed for citric acid warmed at 5K/min. The solid color lines represent the fitted curves for the super-Arrhenius and Arrhenius region. The blue shaded area shows the glass transition region. The two vertical black lines associated with the blue shaded area indicate the corresponding temperature range where the super-Arrhenius curve intersects with the Arrhenius line. The traditional glass transition temperature, i.e., the temperature when $\tau=100$ s, is also marked.

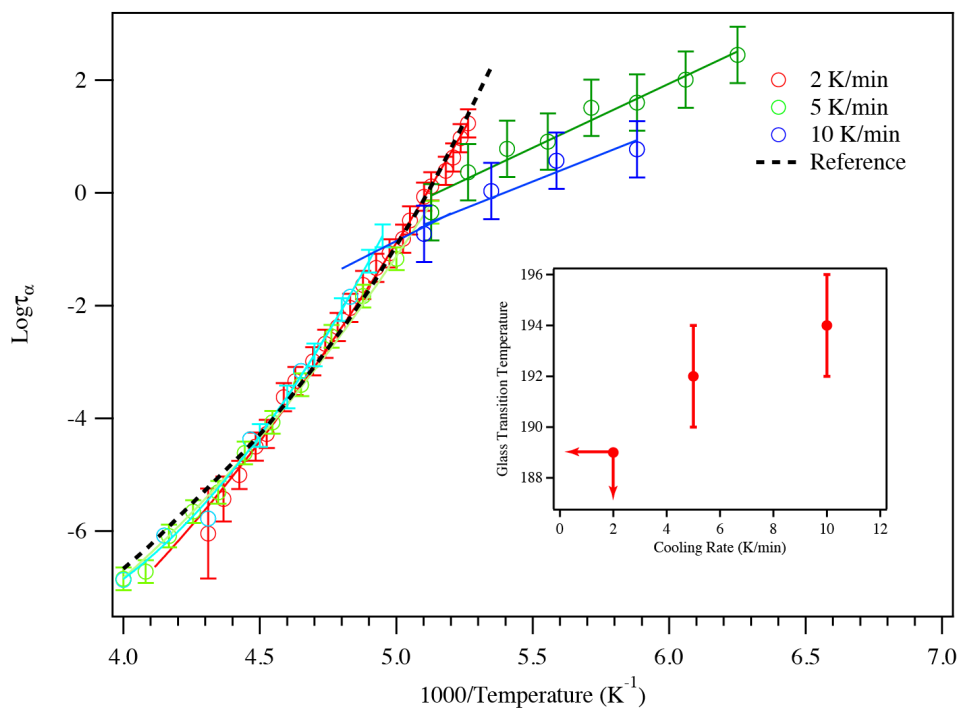


Figure 8. A plot of superimposed data-points and curves constructed for glycerol cooled at 2K/min, 5K/min, and 10K/min. The black dashed line represents literature data of the super-Arrhenius region from Elmatad et al. The open circles are experimental data and the solid lines are fitting results. The inset shows the glass transition temperature of glycerol as a function of cooling rates. At 2 K/min cooling, the glass transition temperature has a higher bound of 189 K.

References

- Adrjanowicz, K., Wojnarowska, Z., Wlodarczyk, P., Kaminski, K., Paluch, M., and Mazgalski, J.: Molecular mobility in liquid and glassy states of Telmisartan (TEL) studied by Broadband Dielectric Spectroscopy, *Eur. J. Pharm. Sci.*, 38, 395-404, <https://doi.org/10.1016/j.ejps.2009.09.009>, 2009.
- Amann-Winkel, K., Gainaru, C., Handle, P. H., Seidl, M., Nelson, H., Böhmer, R., and Loerting, T.: Water's second glass transition, *Proc. Natl. Acad. Sci. USA*, 110, 17720-17725, 10.1073/pnas.1311718110, 2013.
- Bahous, H., Soufi, M. M., Meuret, L., and Benzohra, M.: Relaxation Time at Glass Transition Temperature Measured by Simplex Thermo Stimulated Depolarisation Current, *Macromolecular Symposia*, 341, 45-50, doi:10.1002/masy.201300158, 2014.
- Bateman, A. P., Bertram, A. K., and Martin, S. T.: Hygroscopic Influence on the Semisolid-to-Liquid Transition of Secondary Organic Materials, *J. Phys. Chem. A*, 119, 4386-4395, 10.1021/jp508521c, 2015.
- Beirnes Kimberley, J., and Burns Charles, M.: Thermal analysis of the glass transition of plasticized poly(vinyl chloride), *J. Appl. Polym. Sci.*, 31, 2561-2567, 10.1002/app.1986.070310815, 2003.
- Berkemeier, T., Shiraiwa, M., Pöschl, U., and Koop, T.: Competition between water uptake and ice nucleation by glassy organic aerosol particles, *Atmos. Chem. Phys.*, 14, 12513-12531, 10.5194/acp-14-12513-2014, 2014.
- Bodsworth, A., Zobrist, B., and Bertram, A. K.: Inhibition of efflorescence in mixed organic-inorganic particles at temperatures less than 250 K, *Phys. Chem. Chem. Phys.*, 12, 12259-12266, 10.1039/C0CP00572J, 2010.

Chandler, D., and Garrahan, J. P.: Dynamics on the Way to Forming Glass: Bubbles in Space-Time, *Annu. Rev. Phys. Chem.*, 0, 10.1146/annurev-physchem-61-040610-200001, 2010.

Chen, Z., Sepúlveda, A., Ediger, M. D., and Richert, R.: Dielectric spectroscopy of thin films by dual-channel impedance measurements on differential interdigitated electrode arrays, *Eur. Phys. J. B*, 85, 1-5, 10.1140/epjb/e2012-30363-0, 2012.

Dette, H. P., Qi, M., Schröder, D. C., Godt, A., and Koop, T.: Glass-Forming Properties of 3-Methylbutane-1,2,3-tricarboxylic Acid and Its Mixtures with Water and Pinonic Acid, *J. Phys. Chem. A*, 118, 7024-7033, 10.1021/jp505910w, 2014.

Dette, H. P., and Koop, T.: Glass Formation Processes in Mixed Inorganic/Organic Aerosol Particles, *J. Phys. Chem. A*, 119, 4552-4561, 10.1021/jp5106967, 2015.

Dufour, J., Jorat, L., Bondeau, A., Siblino, A., and Noyel, G.: Shear viscosity and dielectric relaxanion time of dibutyl phthalate down to glass transition temperature, *J. Mol. Liq.*, 62, 75-82, [https://doi.org/10.1016/0167-7322\(94\)00764-0](https://doi.org/10.1016/0167-7322(94)00764-0), 1994.

Elmatad, Y. S., Chandler, D., and Garrahan, J. P.: Corresponding States of Structural Glass Formers, *J. Phys. Chem. B*, 113, 5563-5567, 10.1021/jp810362g, 2009.

Elmatad, Y. S., Chandler, D., and Garrahan, J. P.: Corresponding States of Structural Glass Formers. II, *The Journal of Physical Chemistry B*, 114, 17113-17119, 10.1021/jp1076438, 2010.

Fulcher, G. S.: ANALYSIS OF RECENT MEASUREMENTS OF THE VISCOSITY OF GLASSES, *J. Am. Ceram. Soc.*, 8, 339-355, 10.1111/j.1151-2916.1925.tb16731.x, 1925.

Hallquist, M., Wenger, J. C., Baltensperger, U., Rudich, Y., Simpson, D., Claeys, M., Dommen, J., Donahue, N. M., George, C., Goldstein, A. H., Hamilton, J. F., Herrmann, H., Hoffmann, T., Iinuma, Y., Jang, M., Jenkin, M. E., Jimenez, J. L., Kiendler-Scharr, A., Maenhaut, W., McFiggans, G., Mentel, T. F., Monod, A., Prévôt, A. S. H., Seinfeld, J. H., Surratt, J. D.,

Szmigielski, R., and Wildt, J.: The formation, properties and impact of secondary organic aerosol: current and emerging issues, *Atmos. Chem. Phys.*, 9, 5155-5236, 10.5194/acp-9-5155-2009, 2009.

Hudson, A.: *Statistical Mechanics and Dynamics of Liquids in and out of Equilibrium*, Ph.D., University of California, Berkeley, 2015.

Hudson, A., and Mandadapu, K. K.: On the nature of the glass transition in atomistic models of glass formers, *arXiv*, arXiv:1804.03769, 2018.

Jimenez, J. L., Canagaratna, M. R., Donahue, N. M., Prevot, A. S. H., Zhang, Q., Kroll, J. H., DeCarlo, P. F., Allan, J. D., Coe, H., Ng, N. L., Aiken, A. C., Docherty, K. S., Ulbrich, I. M., Grieshop, A. P., Robinson, A. L., Duplissy, J., Smith, J. D., Wilson, K. R., Lanz, V. A., Hueglin, C., Sun, Y. L., Tian, J., Laaksonen, A., Raatikainen, T., Rautiainen, J., Vaattovaara, P., Ehn, M., Kulmala, M., Tomlinson, J. M., Collins, D. R., Cubison, M. J., E, Dunlea, J., Huffman, J. A., Onasch, T. B., Alfarra, M. R., Williams, P. I., Bower, K., Kondo, Y., Schneider, J., Drewnick, F., Borrmann, S., Weimer, S., Demerjian, K., Salcedo, D., Cottrell, L., Griffin, R., Takami, A., Miyoshi, T., Hatakeyama, S., Shimojo, A., Sun, J. Y., Zhang, Y. M., Dzepina, K., Kimmel, J. R., Sueper, D., Jayne, J. T., Herndon, S. C., Trimborn, A. M., Williams, L. R., Wood, E. C., Middlebrook, A. M., Kolb, C. E., Baltensperger, U., and Worsnop, D. R.: Evolution of organic aerosols in the atmosphere, *Science*, 326, 1525-1529, 2009.

Keys, A. S., Hedges, L. O., Garrahan, J. P., Glotzer, S. C., and Chandler, D.: Excitations Are Localized and Relaxation Is Hierarchical in Glass-Forming Liquids, *Physical Review X*, 1, 021013, 2011.

Keys, A. S., Garrahan, J. P., and Chandler, D.: Calorimetric glass transition explained by hierarchical dynamic facilitation, *Proc. Natl. Acad. Sci. USA*, 110, 4482-4487, 10.1073/pnas.1302665110, 2013.

Koop, T., Bookhold, J., Shiraiwa, M., and Poschl, U.: Glass transition and phase state of organic compounds: dependency on molecular properties and implications for secondary organic aerosols in the atmosphere, *Phys. Chem. Chem. Phys.*, 13, 19238-19255, 2011.

Kuwata, M., and Martin, S. T.: Phase of atmospheric secondary organic material affects its reactivity, *Proc. Natl. Acad. Sci. USA*, 109, 17354-17359, 10.1073/pnas.1209071109, 2012.

Lienhard, D. M., Zobrist, B., Zuend, A., Krieger, U. K., and Peter, T.: Experimental evidence for excess entropy discontinuities in glass-forming solutions, *The Journal of Chemical Physics*, 136, 074515, 10.1063/1.3685902, 2012.

Lienhard, D. M., Huisman, A. J., Bones, D. L., Te, Y.-F., Luo, B. P., Krieger, U. K., and Reid, J. P.: Retrieving the translational diffusion coefficient of water from experiments on single levitated aerosol droplets, *Phys. Chem. Chem. Phys.*, 16, 16677-16683, 10.1039/c4cp01939c, 2014.

Limmer, D. T., and Chandler, D.: Theory of amorphous ices, *Proceedings of the National Academy of Sciences of the United States of America*, 111, 9413-9418, 10.1073/pnas.1407277111, 2014.

Liu, P., Zhang, Y., and Martin, S. T.: Complex refractive indices of thin films of secondary organic materials by spectroscopic ellipsometry from 220 to 1200 nm, *Environ. Sci. Technol.*, 47, 13594-13601, 10.1021/es403411e, 2013.

Lu, Q., and Zografi, G.: Properties of citric acid at the glass transition, *J. Pharm. Sci.*, 86, 1374-1378, 10.1021/js970157y, 1997.

Moynihan, C. T., Eastal, A. J., Wilder, J., and Tucker, J.: Dependence of the glass transition temperature on heating and cooling rate, *The Journal of Physical Chemistry*, 78, 2673-2677, 10.1021/j100619a008, 1974.

Murray, B. J.: Inhibition of ice crystallisation in highly viscous aqueous organic acid droplets, *Atmos. Chem. Phys.*, 8, 5423-5433, 10.5194/acp-8-5423-2008, 2008.

Murray, B. J., Wilson, T. W., Dobbie, S., Cui, Z., Al-Jumur, S. M. R. K., Mohler, O., Schnaiter, M., Wagner, R., Benz, S., Niemand, M., Saathoff, H., Ebert, V., Wagner, S., and Karcher, B.: Heterogeneous nucleation of ice particles on glassy aerosols under cirrus conditions, *Nature Geosci*, 3, 233-237, http://www.nature.com/ngeo/journal/v3/n4/supinfo/ngeo817_S1.html, 2010.

Nakanishi, M., and Nozaki, R.: Dynamics and structure of hydrogen-bonding glass formers: Comparison between hexanetriol and sugar alcohols based on dielectric relaxation, *Physical Review E*, 81, 041501, 2010.

Park, J.-Y., and McKenna, G. B.: Size and confinement effects on the glass transition behavior of polystyrene/o-terphenyl polymer solutions, *Physical Review B*, 61, 6667-6676, 2000.

Price, H. C., Mattsson, J., Zhang, Y., Bertram, A., Davies, J. F., Grayson, J. W., Martin, S. T., O'Sullivan, D., Reid, J. P., Rickards, A. M. J., and Murray, B. J.: Water diffusion in atmospherically relevant [small alpha]-pinene secondary organic material, *Chemical Science*, 10.1039/C5SC00685F, 2015.

Renbaum-Wolff, L., Grayson, J. W., Bateman, A. P., Kuwata, M., Sellier, M., Murray, B. J., Shilling, J. E., Martin, S. T., and Bertram, A. K.: Viscosity of α -pinene secondary organic material and implications for particle growth and reactivity, *Proc. Natl. Acad. Sci. USA*, 110, 8014-8019, 10.1073/pnas.1219548110, 2013.

Richert, R.: Supercooled Liquids and Glasses by Dielectric Relaxation Spectroscopy, in: Adv. Chem. Phys., John Wiley & Sons, Inc., 101-195, 2014.

Rothfuss, N. E., and Petters, M. D.: Characterization of the temperature and humidity-dependent phase diagram of amorphous nanoscale organic aerosols, Phys. Chem. Chem. Phys., 19, 6532-6545, 10.1039/C6CP08593H, 2017.

Saiter, J. M., Grenet, J., Dargent, E., Saiter, A., and Delbreilh, L.: Glass Transition Temperature and Value of the Relaxation Time at T_g in Vitreous Polymers, Macromolecular Symposia, 258, 152-161, doi:10.1002/masy.200751217, 2007.

Shinyashiki, N., Shinohara, M., Iwata, Y., Goto, T., Oyama, M., Suzuki, S., Yamamoto, W., Yagihara, S., Inoue, T., Oyaizu, S., Yamamoto, S., Ngai, K. L., and Capaccioli, S.: The Glass Transition and Dielectric Secondary Relaxation of Fructose–Water Mixtures, J. Phys. Chem. B, 112, 15470-15477, 10.1021/jp807038r, 2008.

Shiraiwa, M., Ammann, M., Koop, T., and Pöschl, U.: Gas uptake and chemical aging of semisolid organic aerosol particles, Proc. Natl. Acad. Sci. USA, 108, 11003-11008, 10.1073/pnas.1103045108, 2011.

Shiraiwa, M., and Seinfeld, J. H.: Equilibration timescale of atmospheric secondary organic aerosol partitioning, Geophys. Res. Lett., 39, L24801, 10.1029/2012GL054008, 2012.

Shiraiwa, M., Li, Y., Tsimpidi, A. P., Karydis, V. A., Berkemeier, T., Pandis, S. N., Lelieveld, J., Koop, T., and Pöschl, U.: Global distribution of particle phase state in atmospheric secondary organic aerosols, Nat. Commun., 8, 15002, 10.1038/ncomms15002 <https://www.nature.com/articles/ncomms15002#supplementary-information>, 2017.

Shrestha, M., Zhang, Y., Upshur, M. A., Liu, P., Blair, S. L., Wang, H., Nizkorodov, S. A., Thomson, R. J., Martin, S. T., and Geiger, F. M.: On surface order and disorder of α -pinene-derived secondary organic material, *J. Phys. Chem. A*, 10.1021/jp510780e, 2014.

Simatos, D., Blond, G., Roudaut, G., Champion, D., Perez, J., and Faivre, A. L.: Influence of heating and cooling rates on the glass transition temperature and the fragility parameter of sorbitol and fructose as measured by DSC, *J. Therm. Anal.*, 47, 1419-1436, 10.1007/BF01992837, 1996.

Tammann, G., and Hesse, W.: Die Abhängigkeit der Viscosität von der Temperatur bei unterkühlten Flüssigkeiten, *Z. Anorg. Allg. Chem.*, 156, 245-257, 10.1002/zaac.19261560121, 1926.

Virtanen, A., Joutsensaari, J., Koop, T., Kannosto, J., Yli-Pirila, P., Leskinen, J., Makela, J. M., Holopainen, J. K., Poschl, U., Kulmala, M., Worsnop, D. R., and Laaksonen, A.: An amorphous solid state of biogenic secondary organic aerosol particles, *Nature*, 467, 824-827, 10.1038/nature09455, 2010.

Vogel, H.: The law of the relation between the viscosity of liquids and the temperature, *Physikalische Zeitschrift*, 22, 645, citeulike-article-id:4001983, 1921.

Wang, Y. Z., Li, Y., and Zhang, J. X.: Scaling of the hysteresis in the glass transition of glycerol with the temperature scanning rate, *J. Chem. Phys.*, 134, 114510, 10.1063/1.3564919, 2011.

Wilson, T. W., Murray, B. J., Wagner, R., Möhler, O., Saathoff, H., Schnaiter, M., Skrotzki, J., Price, H. C., Malkin, T. L., Dobbie, S., and Al-Jumur, S. M. R. K.: Glassy aerosols with a range of compositions nucleate ice heterogeneously at cirrus temperatures, *Atmos. Chem. Phys.*, 12, 8611-8632, 10.5194/acp-12-8611-2012, 2012.

Zhang, Y., Sanchez, M. S., Douet, C., Wang, Y., Bateman, A. P., Gong, Z., Kuwata, M., Renbaum-Wolff, L., Sato, B. B., Liu, P. F., Bertram, A. K., Geiger, F. M., and Martin, S. T.: Changing shapes and implied viscosities of suspended submicron particles, *Atmos. Chem. Phys.*, 15, 7819-7829, 10.5194/acp-15-7819-2015, 2015.

Zhang, Y., Chen, Y., Lambe, A. T., Olson, N. E., Lei, Z., Craig, R. L., Zhang, Z., Gold, A., Onasch, T. B., Jayne, J. T., Worsnop, D. R., Gaston, C. J., Thornton, J. A., Vizueté, W., Ault, A. P., and Surratt, J. D.: Effect of Aerosol-Phase State on Secondary Organic Aerosol Formation from the Reactive Uptake of Isoprene-Derived Epoxydiols (IEPOX), *Environ. Sci. Technol. Lett.*, 5, 167-174, 10.1021/acs.estlett.8b00044, 2018.

Zobrist, B., Marcolli, C., Pedernera, D. A., and Koop, T.: Do atmospheric aerosols form glasses?, *Atmos. Chem. Phys.*, 8, 5221-5244, 10.5194/acp-8-5221-2008, 2008.

Zobrist, B., Soonsin, V., Luo, B. P., Krieger, U. K., Marcolli, C., Peter, T., and Koop, T.: Ultra-slow water diffusion in aqueous sucrose glasses, *Phys. Chem. Chem. Phys.*, 13, 3514-3526, 10.1039/C0CP01273D, 2011.

Zondervan, R., Kulzer, F., Berkhout, G. C. G., and Orrit, M.: Local viscosity of supercooled glycerol near T_g probed by rotational diffusion of ensembles and single dye molecules, *Proc. Natl. Acad. Sci. USA*, 104, 12628-12633, 10.1073/pnas.0610521104, 2007.

1 **SUPPORTING INFORMATION**

2 **Kinetic Controlled Glass Transition Measurement of Organic Aerosol Thin**
3 **Films Using Broadband Dielectric Spectroscopy**

4 Yue Zhang^{1,2,£}, Shachi Katira³, Andrew Lee^{1,†}, Andrew T. Lambe², Timothy B. Onasch^{1,2}, Wen
5 Xu², Manjula R. Canagaratna², Andrew Freedman², John T. Jayne², Doug R. Worsnop², Paul
6 Davidovits^{1,*}, David Chandler^{3,§}, Charles E. Kolb^{2,*}

7

8 *1 Department of Chemistry, Boston College, Chestnut Hill, MA, 02459*

9 *2 Aerodyne Research Inc., Billerica, MA, 01821*

10 *3 Department of Chemistry, University of California, Berkeley, CA, 94720*

11 *£ Now at Department of Environmental Science and Engineering, Gillings School of*

12 *Global Public Health, University of North Carolina at Chapel Hill*

13 *† Now at Department of Chemistry, University of North Carolina at Chapel Hill*

14 *§Deceased April 2017*

15

16

17

18

19

20

21 No. of pages: 2

22 No. of figures: 1

23

24 **Havriliak-Negami Equation and Fitting Principles**

25 The real part of the Havriliak-Negami equation, $\varepsilon'(\omega)$, is shown as:

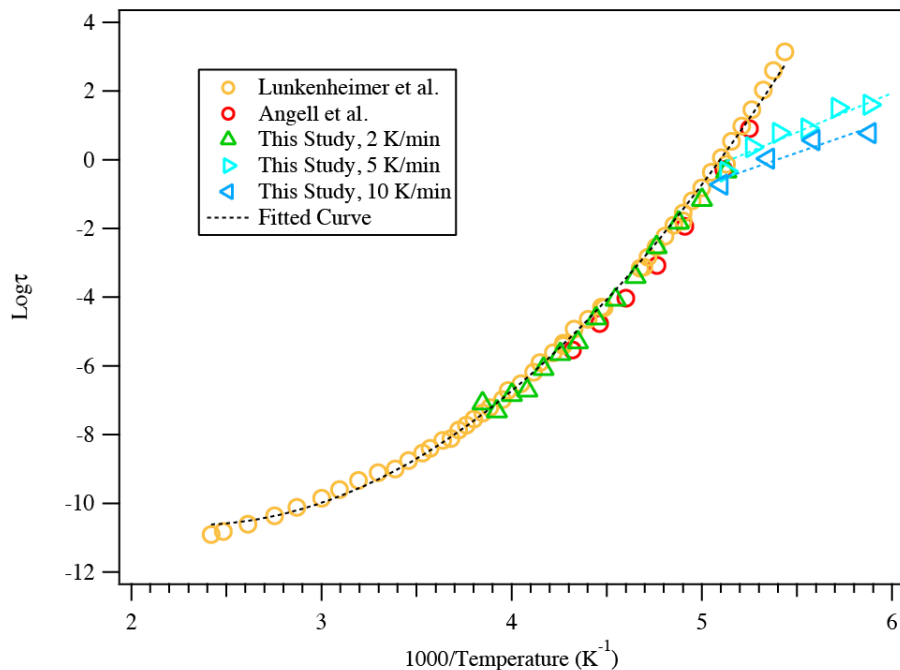
$$26 \quad \varepsilon'(\omega) = \varepsilon_{\infty} + \Delta\varepsilon(1 + 2(\omega\tau)^{\alpha} \cos\left(\frac{\pi\alpha}{2}\right) + (\omega\tau)^{2\alpha})^{-\beta/2} \cos(\beta\varphi) \quad (\text{S1})$$

27 where ε_{∞} is the permittivity at the high frequency limit, α, β are fitting parameters, and τ
28 is the characteristic relaxation time of the medium.

29 The imaginary part of the Havriliak-Negami, $\varepsilon''(\omega)$, is shown in Eq. (2). Sometimes,
30 when there are ionic impurities in the supercooled liquid, a dc-conductivity term that follows
31 strictly through ω^{-1} can contribute to the imaginary part as well (Adrjanowicz et al., 2009). The
32 imaginary part of the of the Havriliak-Negami equation is re-written as:

$$33 \quad \varepsilon''(\omega) = \frac{\sigma_{dc}}{\varepsilon_0\omega} + \Delta\varepsilon(1 + 2(\omega\tau)^{\alpha} \cos\left(\frac{\pi\alpha}{2}\right) + (\omega\tau)^{2\alpha})^{-\beta/2} \sin(\beta\varphi) \quad (\text{S2})$$

34 where σ_{dc} is the conductivity of the supercooled liquid, ε_0 is a permittivity constant.



35

36 **Figure S1.** The logarithm of the relaxation timescale as a function of the inverse temperature
 37 derived from glycerol. The circles are from Lunkenheimer et al. (1999) and Angell (1995). The
 38 triangular points are experimental measurements from this work with different cooling rates. The
 39 dashed lines are the fitted curves for the super-Arrhenius and Arrhenius regions. The results
 40 show that the T_g values from this work match very well with previous studies.

41

42

43 **References**

44 Angell, C. A.: Formation of glasses from liquids and biopolymers, *Science*, 267, 1924-1935,
45 1995.

46 Lunkenheimer, P., Schneider, U., Brand, R., and Loidl, A.: Broadband dielectric response of
47 glycerol and propylene carbonate: a comparison, *AIP Conference Proceedings*, 469, 433-440,
48 10.1063/1.58527, 1999.

49